Centromeric CENP-A loading requires accurate mitotic timing, which is linked to checkpoint proteins

Anne Laure Pauleau[1,2,3], Andrea Bergner[1,2,3], Janko Kajtez[1,4], and Sylvia Erhardt[1,2,3]

[1] Center for Molecular Biology of Heidelberg University (ZMBH), Im Neuenheimer Feld 282, 69120 Heidelberg, Germany.

[2] DKFZ-ZMBH-Alliance, 69120 Heidelberg, Germany.

[3] CellNetworks Excellence Cluster, Heidelberg University, 69120 Heidelberg, Germany.

[4] current address: Department of Micro- and Nanotechnology, Technical University of Denmark, Produktionstorvet 423, DK-2800 Kgs. Lyngby, Denmark.

Correspondence to Sylvia Erhardt: s.erhardt@zmbh.uni-heidelberg.de

Abstract

A defining feature of centromeres is the presence of the histone H3 variant CENP-A that replaces H3 in a subset of centromeric nucleosomes. In *Drosophila* cultured cells CENP-A deposition at centromeres takes place during the metaphase stage of the cell cycle and strictly depends on the presence of its specific chaperone CAL1. How CENP-A loading is restricted to mitosis is unknown. We found that CAL1 interacts with the spindle assembly checkpoint protein and RZZ complex component Zw10 and thus constitutes the anchor for the recruitment of RZZ. We identify Zw10 as determinant of a mitotic duration and show that it is inversely correlated with CENP-A levels at centromeres. Moreover, overexpression of CAL1 is associated with increased CENP-A levels at centromeres and completely uncouples CENP-A loading from mitosis. Therefore CAL1 controls CENP-A incorporation at centromeres both quantitatively and temporally, connecting it to the spindle assembly checkpoint to further ensure mitotic fidelity.

32 **Introduction**

33 The formation of two genetically identical daughter cells with a correct and stable genome is
34 of utmost importance during mitosis. Condensed chromosomes are attached and
35 segregated to the opposing poles of the dividing cell at anaphase by the mitotic spindle. At
36 the interface between the chromosomes and the spindle microtubules lies the kinetochore.
37 This multi-protein complex assembles during mitosis on a specialized domain of the
38 chromosome called centromere, which is defined by an enrichment of nucleosomes
39 containing the histone H3 variant CENP-A, also called CID in *Drosophila*. In many organisms,
40 CENP-A recruits the components of the inner kinetochore components collectively known as
41 CCAN (Constitutive Centromere-Associated Network), which in turn recruit the outer
42 kinetochore components of the KMN network (formed by the Knl1 complex, the Mis12
43 complex and the Ndc80 complex) (Joglekar and Kukreja, 2017). The Ndc80 complex is mainly
44 responsible for connecting microtubules with kinetochores while the Knl1 complex mostly
45 functions to coordinate the Spindle Assembly Checkpoint (SAC) (Musacchio and Desai,
46 2017). The SAC delays entry into anaphase until all chromosomes are properly attached and
47 aligned at the metaphase plate. The metaphase to anaphase transition is controlled by the
48 activation by Cdc20 of the APC/C, a multisubunit ubiquitin ligase that triggers the
49 degradation of cell cycle regulators by the proteasome (Kapanidou et al., 2017). The SAC
50 proteins Mad2, BubR1, and Bub3 sequester Cdc20 forming the Mitotic Checkpoint Complex
51 (MCC) thereby preventing the activation of the APC/C. Finally, the Mis12 complex serves as
52 a hub interacting with all kinetochore complexes as well as with the inner centromere CCAN
53 (Musacchio and Desai, 2017).

54 In some organisms, including *Drosophila melanogaster,* most CCAN proteins cannot be
55 identified with the exception of CENP-C (Westermann and Schleiffer, 2013). CENP-C has
56 been shown to act as a linker between CENP-A nucleosomes and the Mis12 complex
57 (Przewloka et al., 2011). CENP-C is also implicated in CENP-A replenishment at centromeres
58 during mitosis, serving as a platform to recruit the CENP-A chaperone CAL1 (Erhardt et al.,
59 2008). The *Drosophila* outer kinetochore is less complex than in other organisms as several
60 subunits of the KMN network including Mis12 complex subunit Dsn1, Knl1 complex subunit
61 Zwint, and Ndc80 complex subunit Spc24, are absent (Przewloka et al., 2007; Schittenhelm
62 et al., 2007). These changes affect the recruitment of the SAC proteins to the kinetochore
63 and their regulation, and it still remains to be analyzed how the *Drosophila* kinetochore has
64 solved this. In addition to the checkpoint proteins mentioned above, other proteins have
65 been implicated in SAC activity including Bub1, Mad1, the Mps1 and Aurora B kinases and
66 the RZZ complex (formed by the three proteins Rough Deal (ROD), Zw10 and Zwilch)
67 (Musacchio, 2015). In *Drosophila*, BubR1 and Bub1 localization to the kinetochore partly
68 depends on Spc105R (Schittenhelm et al., 2009), while Mad1 and Mad2 rely on the previous
69 recruitment of the RZZ complex (Buffin et al., 2005; Defachelles et al., 2015b). The RZZ
70 complex is conserved in all metazoans (Karess, 2005; Schmitt, 2010; Vleugel et al., 2012).
71 Besides Mad1-Mad2, RZZ also recruits Spindly and the motor protein Dynein, thereby being
72 essential for SAC silencing (Gassmann et al., 2008; Griffis et al., 2007; Starr et al., 1998;
73 Wojcik et al., 2001). Moreover, a recent study has shown that kinetochore size regulation
74 and maturation depends on RZZ and Spindly (Sacristan et al., 2018). RZZ recruitment to the
75 kinetochore at prometaphase has been shown to be mediated by KNL1 and Zwint in higher
76 eukaryotes (Caldas et al., 2015; Kasuboski et al., 2011) but no such dependency exist in
77 *Drosophila*. Therefore, we set out to identify the RZZ receptor in *Drosophila*. In the course of

78 these studies we found a surprising interaction of the RZZ complex with constitutive inner
79 kinetochore components and the loading machinery of CENP-A. Strikingly, we discovered a
80 co-dependence of mitotic duration and accurate CENP-A loading that seems mediated by
81 the interaction with these checkpoint proteins. Importantly, experimentally changing the
82 duration of mitosis affects CENP-A loading during mitosis, whereas increasing the pool of its
83 loading factor CAL1 uncouples CENP-A loading from mitosis. These data suggest an intricate
84 coordination of SAC, CENP-A loading, and mitotic duration.
85
86 **Results**
87 **Zw10 mediates the recruitment of the RZZ to the kinetochore independently of Spc105R.**
88 How RZZ is recruited to the kinetochore at mitosis onset remains elusive in *Drosophila*. We
89 first sought to determine if one of the RZZ components is responsible for targeting the
90 whole complex to the kinetochore. The RZZ complex is a conserved complex composed of
91 the three proteins, Rough Deal (ROD), Zwilch and Zw10 (Barisic and Geley, 2011; Karess,
92 2005; Schmitt, 2010). We established S2 cell lines stably expressing GFP-tagged ROD, Zwilch,
93 or Zw10 and found that the localization of these tagged proteins is in accordance with
94 endogenous proteins (Scaerou et al., 1999; Williams et al., 1992; Williams et al., 2003) as
95 well as transgenes expression (Basto et al., 2004; Buffin et al., 2005; Defachelles et al.,
96 2015b) reported in Drosophila tissues: GFP-Zw10 located in the cytoplasm during interphase
97 whereas low levels of GFP-Zwilch and GFP-ROD could be detected in the cytoplasm during
98 interphase (Fig. S1A-C). Following the disassembly of the nuclear envelope at the onset of
99 mitosis all three proteins were recruited to the kinetochore where they remained until
100 complete chromosome biorientation. RZZ proteins were then transported along the spindle
101 microtubules (Fig. S1A-C) in a process mediated by Spindly and Dynein required to silence

102 the SAC (Gassmann et al., 2008; Griffis et al., 2007; Starr et al., 1998; Wojcik et al., 2001).
103 Knockdown of all RZZ complex components (Fig. S1D-E) led to the known spindle
104 morphology defects in all cell lines (Fig. 1A-B) (Defachelles et al., 2015a; Karess and Glover,
105 1989; Williams et al., 1992; Williams et al., 2003). Importantly, depletion of any complex
106 component led to a reduction of the other GFP-RZZ proteins at kinetochores (Fig. 1A-B)
107 suggesting that the RZZ components are mutually dependent on each other similar to what
108 has been reported in Drosophila tissues (Defachelles et al., 2015a; Scaerou et al., 2001;
109 Wainman et al., 2012; Williams and Goldberg, 1994; Williams et al., 2003)(Fig. 1A).
110 However, levels of GFP-Zw10 at kinetochores were usually the least affected indicating that
111 some GFP-Zw10 is still recruited to kinetochores in absence of its complex partners ROD or
112 Zwilch (Fig. 1A-B). These data suggest that Zw10 may be the most proximal component of
113 the complex at kinetochores in Drosophila cells.
114
115 In mammalian cells, the recruitment of the RZZ complex depends on the presence of KNL1
116 and Zwint at kinetochores (Kops et al., 2005; Starr et al., 2000). As no ortholog of Zwint has
117 been identified in *Drosophila* so far, we tested if the *Drosophila* KNL1 ortholog Spc105R is
118 required for RZZ recruitment to the kinetochore. Depletion of Spc105R (Fig. S1D) did not
119 affect Zw10 localization (Fig. 1C-D). Reciprocally, depletion of Zw10 (Fig.S1D) did not
120 prevent Spc105R localization at the kinetochore (Fig. S2A-B). We then tested Mis12 (Fig.
121 S1D), which has been shown to localize to kinetochores throughout the cell cycle (Przewloka
122 et al., 2007) and found that it is also not involved in Zw10 recruitment to the kinetochore
123 (Fig. 1E-F). Therefore, we propose that the *Drosophila* checkpoint proteins and outer
124 kinetochore components are assembled through two independent branches: on the one
125 hand the RZZ complex, which is necessary to localize the MAD proteins to the kinetochore

126 (Buffin et al., 2005), and on the other hand Mis12-Spc105R, which are required to recruit all
127 others components of the KMN network as well as the BUB proteins (Basu et al., 1998; Orr
128 and Sunkel, 2010; Przewloka et al., 2007; Schittenhelm et al., 2009).
129
130 **RZZ recruitment to the kinetochore requires direct interaction with inner centromere**
131 **components.**
132 Like all kinetochore proteins tested so far (Przewloka et al., 2007), the localization of Zw10
133 to the kinetochore is abolished when the inner centromere protein CENP-A (Fig. 2A-B)
134 and/or its loading factor CAL1 (Fig. S2C) are depleted even though Zw10 protein levels
135 remained largely unchanged in Western blot analysis (Fig. S1E). Importantly, CENP-A and
136 CAL1 co-immunoprecipitated with GFP-Zw10 (Fig. 2C). Although we could observe GFP-ROD
137 by immunofluorescence, we were unable to detect it by immunoblotting precluding analysis
138 of ROD immunoprecipitate complexes. Regarding GFP-Zwilch we obtained inconsistent
139 results: CAL1 and CENP-A were immunoprecipitated in some but not all experiments. Zw10
140 is also known to form a complex with the *Drosophila* RINT1 at the Golgi during interphase
141 (Wainman et al., 2012) (Fig. S2D). We observed that GFP-RINT1 immunoprecipitated with
142 Zw10 but neither with CAL1 nor CENP-A indicating that there are, indeed, two Zw10-
143 containing complexes and that Zw10 interacts with CENP-A and CAL1 when it is in a complex
144 with Zwilch and ROD in mitosis (Fig. 2C). To confirm these results, we performed Yeast-two-
145 hybrid (YTH) experiments that repeatedly showed that Zw10 weakly but consistently binds
146 to full length CAL1 and CENP-A (Fig. 2D). Since YTH interaction are often challenging with
147 bigger proteins, we repeated the YTH analysis with yeasts expressing fragments of CAL1 and
148 Zw10 and identified strong interactions of the C-terminus (amino acids 680-979) of CAL1
149 and the C-terminus of Zw10 (amino acids 482-721) (Fig.S2E-F). The C-terminus of CAL1 also

150 binds CENP-C and Roadkill (Bade et al., 2014; Schittenhelm et al., 2010). No further
151 interactions were detected between the other components of the complex and the
152 centromeric proteins supporting our previous observation that Zw10 might be responsible
153 for targeting the RZZ complex to the kinetochore.
154
155 **Zw10 affects the loading of newly synthesized CENP-A during mitosis.**
156 A prominent function of the RZZ complex is to recruit the MAD proteins to the kinetochore,
157 thereby making the RZZ essential for the SAC (Buffin et al., 2005). SAC activity peaks in
158 prometaphase when CENP-A incorporation into centromeric chromatin takes place in
159 *Drosophila* cells (Mellone et al., 2011). Therefore, we sought to identify a possible link
160 between SAC activity and CENP-A loading. We used the SNAP-tag technology (Jansen et al.,
161 2007) in a quench-chase-pulse experiment to label newly synthesized and incorporated
162 CENP-A. At day 3 of Zw10 RNAi, we quenched existing SNAP-CENP-A molecules with a non-
163 fluorescent dye, cultured the cells for 24 hours to allow approximately one additional cell
164 division, then marked newly synthesized SNAP-CENP-A molecules with a fluorophore and
165 measure fluorescent intensity of newly incorporated SNAP-CENP-A at centromeres (Fig. 3A).
166 We found that Zw10 depletion led to a 30% reduction of newly synthesized SNAP-CENP-A
167 (Fig. 3A-B) and SNAP-CAL1 (Fig. S3A-B) at centromeres compared to control-depleted cells.
168 This significant decrease of SNAP-CENP-A centromeric levels may be caused either by a
169 decreased stability or by decreased loading. Since stability of centromeric SNAP-CENP-A was
170 not affected by Zw10 depletion as determined by SNAP-tag pulse chase experiment (Fig.
171 S3C-D), we hypothesized that Zw10 depletion interferes with SNAP-CENP-A loading directly.
172

173 To address a potential role of Zw10 in mitotic loading of CENP-A we measured Fluorescence
174 Recovery After Photobleaching (FRAP) of CENP-A, on the assumption that fast recovery of
175 the signal at centromeres corresponds to active loading of CENP-A. We partially bleached
176 GFP-CENP-A signal during prophase and followed recovery of the signal at centromeres until
177 anaphase. We observed a partial recovery of GFP-CENP-A at centromeres in control cells
178 confirming previous reports that loading of new CENP-A takes place during mitosis (Mellone
179 et al., 2011) (Fig. 3C). Importantly, the recovery rate of GFP-CENP-A at centromeres was
180 comparable in control and Zw10-depleted cells (Fig. 3D-E). Thus, the CENP-A mitotic loading
181 machinery seemed functional in Zw10-depleted cells and does not explain the observed
182 impaired loading of CENP-A.
183
184 Besides mitotic loading, additional CENP-A loading has been reported in G1 in S2 cells
185 (Lidsky et al., 2013). We, therefore, followed cells through mitosis, partially bleached GFP-
186 CENP-A in early G1 and measured GFP-CENP-A signal intensity for 3 hours but did not detect
187 any recovery of the bleached GFP-CENP-A signal (Fig. S3E-F). We explained these results
188 with a likely absence of any active and measurable CENP-A loading in early G1. Strikingly,
189 however, during the course of these live cell analyses we noticed that Zw10-depleted cells
190 displayed a shorter mitosis compared to control cells (Fig. 3C). This result is in accordance
191 with the Premature Sister Chromatids Separation (PSCS) phenotype observed in Zw10
192 mutant embryos and larval tissues (Basto et al., 2000; Scaerou et al., 1999; Williams et al.,
193 1992).
194
195 **CENP-A loading correlates with mitosis duration.**

196 To confirm that Zw10-depleted cells proceed faster through mitosis, we performed time-
197 lapse microscopy analysis of cells stably expressing H2B-GFP and mCherry-Tubulin. Indeed,
198 mitotic timing (defined as the time that elapses between late prophase (determined by the
199 partial nuclear envelop breakdown (NEB) concomitant with the formation of two spindle
200 poles) and anaphase entry) was significantly shorter in Zw10-depleted cells than in control
201 cells (Fig. 4A-B; videos 1-2). This raised the possibility that decreased SNAP-CENP-A
202 incorporation in Zw10-depleted cells could be a consequence of a shortened mitosis. To test
203 this, we depleted two other mitotic checkpoint proteins, Mad2 and BubR1, known to reduce
204 mitosis duration (Lince-Faria et al., 2009; Orr et al., 2007; Rahmani et al., 2009). These
205 depletions (Fig. S4A) also led to a decrease of newly synthesized centromeric SNAP-CENP-A
206 incorporation similar to Zw10 depletion (Fig. 4C-D). On the contrary, depletion of Mis12 (Fig.
207 S4A), which has been previously shown not to affect duration of mitosis in Drosophila
208 cultured cells (Feijao et al., 2013), did not alter SNAP-CENP-A amount at centromeres (Fig.
209 4C-D). Therefore, we hypothesized that the amount of newly synthesized CENP-A that can
210 be incorporated into centromeric chromatin depends on mitosis duration. Yet, extending
211 metaphase duration by preventing entry into anaphase through depletion the APC/C
212 cofactor Cdc27 (Huang and Raff, 2002) or Spindly (required for silencing of the SAC) (Griffis
213 et al., 2007) (Fig. S4A) did not cause an increase of CENP-A levels at centromeres when
214 compared to control (Fig. 4C-D). Arrest in prometaphase by the microtubule-depolymerizing
215 drug Nocodazole or in metaphase by the proteasome inhibitor MG132 also did not cause
216 changes in loading of newly synthesized SNAP-CENP-A (Fig. S4B-C). SNAP-CAL1 centromeric
217 loading was similarly affected: an acceleration of mitotic timing by BubR1 or Mad2 RNAi let
218 to a decrease of loading, whereas mitotic arrest by Cdc27 or Spindly RNAi did not affect
219 loading (Fig. S4D). This set of experiments suggests that the amount of new CENP-A

220 molecules that are incorporated into centromeric chromatin is limited at each round of
221 mitosis. Importantly, FRAP analysis revealed an inverse correlation between CENP-A
222 incorporation rate and mitosis duration in control cells (Fig. 4E), which suggested that either
223 CENP-A loading or CENP-A centromeric levels directly controls the duration of mitosis.
224
225 **CENP-A levels correlate with mitosis duration.**
226 To test if there is a direct correlation between centromeric CENP-A levels and mitosis length
227 we needed an experimental system that reduces CENP-A levels without arresting the cells in
228 mitosis due to the known phenotypes associated with CENP-A depletion (e.g. chromosome
229 segregation defects) that are impedimental to study mitosis progression (Blower and
230 Karpen, 2001). Therefore, we performed CENP-A RNAi depletion in GFP-CENP-A
231 overexpressing cells. Interestingly, depletion of CENP-A in GFP-CENP-A cells led to
232 undetectable levels of endogenous CENP-A but left sufficient GFP-CENP-A to allow some
233 cells to go through mitosis (Fig. 5A-B). As hypothesized, mitosis duration was extended in
234 CENP-A-reduced cells in comparison to control cells (Fig. 5B-C; videos 3-4) as observed in
235 CENP-A mutant fly embryos (Blower et al., 2006), supporting our hypothesis that CENP-A
236 levels might control mitotic length.
237
238 We next sought to determine if elevated CENP-A levels could also influence mitosis
239 duration. However, upregulation of CENP-A to high levels is associated with ectopic CENP-A
240 incorporation into chromosome arms and subsequent defects in mitosis (Heun et al., 2006).
241 In order to avoid this secondary effect, we induced CENP-A overexpression from pMT-CENP-
242 A-GFP plasmid with a short and very low $CuSO_4$ pulse. Under those conditions, CENP-A-GFP
243 was over-expressed while endogenous CENP-A levels were unaffected (Fig. 5D). However,

244 22 hours after the low $CuSO_4$ pulse endogenous CENP-A was almost undetectable, indicating
245 that the cell compensate ectopic CENP-A overexpression by decreasing its endogenous
246 counterpart (Fig. 5D). We also observed a reduction of endogenous CENP-A in cells
247 expressing constitutively GFP-CENP-A and SNAP-CENP-A (Fig. 5D). Under these conditions,
248 non-centromeric CENP-A was undetectable and CENP-A-GFP localized to centromeres (Fig.
249 5E). Using time-lapse analysis we found that the cells with a mild increase of CENP-A
250 progressed significantly faster through mitosis (Fig. 5G-H; videos 5-6). Importantly we
251 observed no increase in mitotic defects usually associated with CENP-A overexpression such
252 as chromosomes misalignment and lagging chromosomes (Fig 5I). Together these results
253 confirm our hypothesis that centromeric CENP-A levels influence mitosis duration.
254
255 **CAL1 levels regulate the amount of CENP-A at centromere.**
256 To confirm our observations that CENP-A levels influences mitosis duration, we sought to
257 manipulate CENP-A indirectly. Centromeric CENP-A loading is mediated by its loading factor
258 CAL1 (Chen et al., 2014; Erhardt et al., 2008). In addition, CAL1 has been shown to be the
259 limiting factor of CENP-A incorporation in flies (Schittenhelm et al., 2010). We
260 overexpressed CAL1 in S2 cells from a $CuSO_4$-inducible pMT promoter and observed an
261 increase of both, endogenous and overexpressed CENP-A (GFP-CENP-A, SNAP-CENP-A)
262 levels (Fig. 6A). Overexpressed CAL1 primarily localized to centromeres and the nucleolus
263 similarly to the endogenous protein (84 % of cells showing CAL1-V5). Cytoplasmic and/or
264 nucleoplasmic CAL1 were visible in about 15 % of the cells but CENP-A was only localized to
265 centromeres (Fig. 6B) and was not detectable at any other chromatin regions on metaphase
266 chromosomes (Fig. 6C). This result indicates that CAL1 overexpression alone does not lead
267 to ectopic incorporation of CENP-A. Importantly, however, and in contrast to previous

268 observations in embryos (Schittenhelm et al., 2010), centromeric CENP-A levels were
269 massively increased, up to 200%, after 24 hours of CAL1 overexpression (Fig. 6D).
270 Surprisingly, CENP-C levels remained largely unaffected by CAL1 overexpression (Fig. 6E-F).
271 These results show that the centromeric amount of CENP-A is regulated by the available
272 amount of CAL1. To test whether the increased CENP-A level is due to more CENP-A loading
273 we overexpressed CAL1 in SNAP-CENP-A expressing cells and measured incorporation of
274 newly synthesized CENP-A. As expected, significantly more SNAP-CENP-A incorporated into
275 centromeres in CAL1 overexpressing cells (Fig. 6G-H). These data confirm that CENP-A
276 centromeric levels are regulated by CAL1 and that CAL1 overexpression specifically
277 increases incorporation of newly synthesized CENP-A in centromeric chromatin.
278
279 **Overexpression of CAL1 leads to centromeric CENP-A loading outside of mitosis.**
280 Since CAL1 overexpression is suitable to study the effect of CENP-A levels on mitosis
281 duration we performed time-lapse microscopy experiments on CAL1-overexpressing cells
282 and, indeed, found that they proceed faster through mitosis compared to control cells (Fig.
283 7A-B; videos 7-8). Of note, CAL1 overexpressing cells did neither exhibit more mitotic
284 defects (Fig. S5A) nor did they recruit more endogenous kinetochore proteins (CENP-C,
285 Spc105R, BubR1) during prometaphase (Fig. S5B). CAL1-overexpressing cells also display a
286 functional SAC because cells treated with the microtubule interfering drug Taxol triggered a
287 cell cycle arrest in prometaphase in control cells as well as in CAL1-overexpressing cells (Fig.
288 S5C-D). We concluded that CAL1-overexpressing cells not only incorporated more CENP-A at
289 centromeres, they also progressed faster through mitosis.
290

291 To determine if CAL1 overexpression accelerates CENP-A loading during mitosis, we
292 performed FRAP experiments and measured the recovery rate of GFP-CENP-A after
293 photobleaching in prophase. Surprisingly, GFP-CENP-A recovery rate decreased in CAL1-
294 overexpressing cells as compared to control cells (Fig. 7C-D). In addition, the inverse
295 correlation that we observed in control cells between CENP-A incorporation rate at
296 centromeres and mitosis duration was not preserved in CAL1-overexpressing cells. This
297 suggests that rather than the rate of incorporation, the amount of CENP-A itself correlates
298 with mitosis duration in control cells.
299
300 Since the availability of CAL1 seems to be the crucial aspect for CENP-A incorporation, we
301 tested if CAL1-misexpressing cells incorporate CENP-A into centromeric chromatin outside
302 mitosis. Thus, we arrested cells at the metaphase to anaphase transition using MG132
303 treatment for 2 hours, blocked existing SNAP-CENP-A molecules using SNAP-Block and
304 cultured the cells for an additional 4 hours in the presence of MG132 (Fig. S6A) similar to a
305 previously published protocol (Mellone et al., 2011). Whereas we observed about 10%
306 SNAP-CENP-A loading in uninduced pMT-CAL1 cells, the induction of pMT-CAL1 and
307 resulting overexpression of CAL1 let to an incorporation of newly synthesized SNAP-CENP-A
308 in about 40% of the cells pointing to loading outside of mitosis (Fig. S6A). To further confirm
309 that overexpressed CAL1, indeed, loads CENP-A to centromeres outside of mitosis, we
310 followed newly synthesized SNAP-CENP-A live by time-lapse microscopy. We blocked
311 existing SNAP-CENP-A with SNAP-Block, washed and added SNAP-640 fluorophore
312 (Butkevich et al., 2017) to the culture medium in order to stain newly synthesized SNAP-
313 CENP-A molecules. Despite some aggregation of the dye, SNAP-CENP-A loading at
314 centromeres was discernable in both, CAL1 overexpressing and control cells. We only

315 analyzed cycling cells that eventually entered mitosis during the course of imaging and
316 determined whether and when they incorporated SNAP-CENP-A. We found that in the
317 uninduced control cells 38% had SNAP-CENP-A signals at centromeres by the end of the
318 imaging (Fig. 7E-F; videos 9). Of those, 91 % loaded SNAP-CENP-A during mitosis and 9%
319 after the cell exited mitosis. In contrast, 81% of cycling CAL1-overexpressing cells had SNAP-
320 CENP-A signals at centromeres (Fig. 7E-F; videos 10), and of those 31% loaded before
321 mitosis and 51% after the cells exited of mitosis. The specificity of the signal was verified by
322 co-staining with anti-CENP-A antibody immediately after block (0 min), and 20 hours of
323 incubation with SNAP-640 (Fig. S6B). No SNAP-CENP-A was detected directly after SNAP-
324 block treatment, confirming the efficient quenching of old SNAP-CENP-A molecules (Fig.
325 S6B). After 20 hours newly synthesized SNAP-CENP-A perfectly co-localized with total CENP-
326 A signals at centromeres. Interestingly, when we counted the percentage of cells that
327 displayed SNAP-CENP-A at centromeres in these fixed samples we did not observe any
328 differences between control and CAL1-overexpressing cells after 20 h (Fig. S6C). However,
329 SNAP-CENP-A centromeric intensity was four times higher in CAL1-overexpressing cells than
330 in control cells (Fig. S6D). This suggests that low SNAP-CENP-A protein levels were masked in
331 the presence of excess SNAP dye in live cell analysis. Nevertheless, the analysis of SNAP-
332 CENP-A loading in cycling cells revealed that cells overexpressing CAL1 loaded CENP-A
333 throughout the cell cycle while loading outside mitosis did not occur in control cells (Fig.
334 7G). In conclusion, overexpression of the CENP-A-specific chaperone CAL1 uncouples CENP-
335 A centromeric loading from mitosis and leads to an uncontrolled overload of CENP-A at
336 centromeres that is usually prevented by a crosstalk with the SAC and the length of mitosis.
337

338 **Discussion**

339 Many central components of the spindle assembly checkpoint require outer kinetochore
340 components for their localization to centromeric regions. In yeast and worms, for instance,
341 Mad1/2 recruitment depends on KNL1 (London and Biggins, 2014; Moyle et al., 2014), in
342 other eukaryotes, Mad1/Mad2 recruitment to the kinetochore also requires the RZZ
343 complex (Caldas et al., 2015; Kops et al., 2005; Silio et al., 2015). In mammalian cells, RZZ
344 recruitment to the kinetochore depends on Bub1, which itself requires KNL1/Zwint (Caldas
345 et al., 2015; Varma et al., 2013; Zhang et al., 2015) although experimental results suggest
346 the existence of a KNL1-independent mechanism (Caldas et al., 2015; Petsalaki et al., 2018;
347 Silio et al., 2015). In *Drosophila*, many outer kinetochore components are missing
348 (Przewloka et al., 2007; Schittenhelm et al., 2007) and even though Mad1/2 recruitment to
349 the kinetochore also depends on the RZZ complex (Buffin et al., 2005) the factors necessary
350 for the localization of the RZZ to kinetochores and whether RZZ and spindly are required for
351 kinetochore expansion remain elusive (Sacristan et al., 2018). In this paper we show that
352 RZZ localization to the kinetochores does not require KNL1^{Spc105R} but depends on the inner
353 kinetochore proteins CAL1 and CENP-A. Therefore, we hypothesize that the *Drosophila*
354 outer kinetochore and components of the SAC assemble through two independent
355 pathways: the CENP-C-KMN-Bub1-Bub3/BubR1 branch (Basu et al., 1998; Przewloka et al.,
356 2011; Schittenhelm et al., 2009) or the here described CAL1-RZZ-Mad1/2 branch. How those
357 two pathways interconnect for the formation of MCC complexes remains to be determined.
358 One link may be the KMN complex, since Mad2 has been shown to be diminished in the
359 absence of KMN proteins (Feijao et al., 2013). Interestingly, Spc105R mutation does not
360 affect SAC function in fly embryos suggesting that flies rely more on the RZZ-Mad1/2 branch
361 to engage the SAC (Schittenhelm et al., 2009).

362

363 We show here that CAL1 binds to Zw10 through its C-terminus, the same region required for
364 its interaction with CENP-C (Schittenhelm et al., 2010) and the E3 ligase adaptor Roadkill
365 (Bade et al., 2014). On the other hand, no binding partner of CAL1 N-terminal region other
366 than CENP-A has been identified so far. This suggests that, while the interaction between
367 CAL1 and CENP-A is very stable, the C-terminal interacting partners of CAL1 are potentially
368 of regulatory nature and more versatile, as one would expect for component of the SAC.

369 In *Drosophila* cells, CENP-A loading primarily takes place during prometaphase-metaphase
370 (Mellone et al., 2011). Additional turnover of CENP-A in G1 has been reported leading to the
371 hypothesis that CENP-A could be further incorporated at this stage (Lidsky et al., 2013). We
372 did not observe any CENP-A turnover during early G1 in our FRAP experiments when we
373 bleached centromeric CENP-A at the end of cytokinesis. However, our FRAP experiments
374 and our live staining of newly synthesized SNAP-CENP-A confirmed the observations
375 reported by Mellone et al., that the majority of CENP-A loading takes place during mitosis in
376 *Drosophila* cultured cells (Mellone et al., 2011).

377 With SNAP-tagged CENP-A we showed that centromeric loading of newly synthesized CENP-
378 A was decreased in Zw10-deficient cells even though the loading machinery for CENP-A
379 mitotic incorporation was functional in these cells. Importantly, we found that Zw10 affects
380 the length of mitosis allowing sufficient time for chromosomes to attach and align. Since
381 CENP-A loading occurs during this time window, we investigated a possible link between
382 CENP-A loading and mitotic timing. Indeed, shortening mitosis duration through the
383 depletion of the two proteins Mad2 and BubR1 previously shown to affect mitosis duration
384 (Meraldi et al., 2004) recapitulated the decreased CENP-A loading observed after Zw10
385 depletion strongly arguing that mitosis duration affects CENP-A loading. Elongating the

386 mitotic time window during which CENP-A is usually loaded (Spindly, Cdc27 depletion or by
387 drug treatment) did not increase the amount of CENP-A incorporated at centromeres,
388 showing that only a defined amount of CENP-A can be incorporated at each mitosis. How
389 CENP-A levels at centromeres are sensed is unclear; one model is that BubR1 and Mad2
390 function as mitotic timer (Buffin et al., 2007; Lince-Faria et al., 2009; Meraldi et al., 2004;
391 Rahmani et al., 2009) and we could envision a role of Zw10 in this process. Mad2 but not
392 Mad1 has been shown to be a central determinant of the mitotic timing (Emre et al., 2011;
393 Meraldi et al., 2004), leading to the hypothesis that cytosolic Mad2-Cdc20 complexes form
394 independently of Mad1 and determine the timing of mitosis (Emre et al., 2011; Li et al.,
395 2017). It has previously been proposed that low CENP-A levels at centromeres lead to more
396 cytosolic Mad2 thereby keeping the timer active longer (Blower et al., 2006). We
397 hypothesized that higher CENP-A levels at centromeres during early mitosis would
398 accelerate the recruitment of RZZ and consequently Mad2 to the kinetochores, therefore,
399 releasing the timer and shortening mitosis duration in cells where kinetochores attach
400 properly to the spindle microtubules. Interestingly, Nocodazole treatment did not affect
401 CENP-A loading confirming previous observations that kinetochores attachment to the
402 microtubule spindle does not play a role in CENP-A loading (Mellone et al., 2011). These
403 results are pointing further to an additional function of the SAC independent of the control
404 of microtubule attachment. However, recent evidence show that RZZ together with Spindly
405 plays a central role in kinetochore expansion during early mitosis to form a fibrous corona
406 that then compacts upon microtubule capture (Sacristan et al., 2018). How this plays a role
407 in CENP-A loading needs to be investigating.

408

409 In flies, CENP-A incorporation is controlled by its chaperone CAL1 (Chen et al., 2014; Erhardt
410 et al., 2008; Schittenhelm et al., 2010). We found that overexpression of CAL1 leads to
411 increased CENP-A protein levels but Chen et al., previously reported that CAL1-GFP-LacI
412 overexpression alone did not affect CENP-A when targeted to an exogenous LacO array
413 (Chen et al., 2014). Under our conditions, CAL1-V5 was strongly overexpressed and caused
414 an intense centromeric and nucleolar localization of CAL1 and a centromere-specific
415 overload of CENP-A. Importantly, however, ectopic incorporation of CENP-A was never
416 observed further enhancing the evidence that CAL1 loads CENP-A exclusively to
417 centromeres. Important for our study is that the increased centromeric CENP-A levels
418 following CAL1 overexpression correlated with faster mitosis. A similar acceleration of
419 mitotic timing was observed when CENP-A was overexpressed in a controlled manner that
420 did not lead to massive incorporation at ectopic sites.

421 The live analysis of newly synthesized CENP-A allowed us to visualize CENP-A incorporation
422 during mitosis. CAL1-overexpressing cells loaded CENP-A in all stages of the cell cycle. This
423 strongly suggests that CAL1's availability and protein amount control CENP-A incorporation
424 into centromeric chromatin both quantitatively and temporally. CENP-A expression (Ahmad
425 and Henikoff, 2001) and its stability (Bade et al., 2014; Moreno-Moreno et al., 2006)
426 together with its dependence on the low abundant and highly specific loading factor CAL1
427 and the here shown connection to mitotic events are likely interconnected cellular
428 surveillance mechanisms to avoid misincorporation of CENP-A and, therefore, securing
429 genome stability. How CAL1 itself is regulated to obtain such specificity is currently
430 unknown. In conclusion, we show that there is a direct crosstalk between the SAC and the
431 maintenance of centromeric chromatin, ensuring mitotic fidelity not only by controlling
432 microtubule attachment but also by regulating accurate composition of centromeres.

433

434 **Materials and methods**

435 **Gene constructs**

436 Plasmid encoding CENP-A tagged with a N-terminal EGFP has been described previously
437 (Erhardt et al., 2008) as well as those encoding CENP-A and CAL1 with N-terminal SNAP tag
438 (Mellone et al., 2011). Constructs created for this study (GFP-ROD, GFP-Zwilch, GFP-Zw10,
439 GFP-RINT1) were cloned into AscI and PacI sites of the pCopia–localization and purification
440 (LAP) vector with a basal expression Copia promoter and an N-terminal mEGFP tag (Erhardt
441 et al., 2008). For overexpression studies, CAL1-V5 and CENP-A-GFP were cloned into pMT
442 vector (Invitrogen). For yeast two hybrid studies, pMM6 plasmids containing full length
443 CAL1, CAL1 truncations and CENP-A have been described in (Bade et al., 2014). Zw10 (full
444 length, aa1-240, aa241-481, aa482-721), Zwilch and Rod (full length, aa1-696, aa697-1392,
445 aa1393-2090) were cloned into pMM5 plasmids.

446 **Cell culture**

447 Cell maintenance

448 *Drosophila* S2 cells were maintained under sterile conditions at 25 °C in Schneider medium
449 containing 10 % heat-inactivated fetal bovine serum (FBS) and 100 µg/ml
450 Penicillin/Streptomycin. Expression of genes under the metallothionein promoter (pMT
451 vector) was induced by supplementing the medium with $CuSO_4$ (CENP-A-GFP: 10 µM; CAL1-
452 V5: 100 µM).

453 RNAi and Transfection Experiments

454 Double-stranded RNA (dsRNA) was produced using the MEGAscript (Ambion) kit according
455 to the manufacturer's protocol. RNAi was carried out as described previously (Erhardt et al.,

456 2008). In short, 10^6 S2 cells were incubated for 1 h with 15 µg dsRNA in serum-free medium.
457 Subsequently, 2 volumes of 15 % serum containing medium were added. Analysis was
458 usually performed 96 h after treatment.
459 Stable cell lines were generated by co-transfecting the plasmid of interest together with a
460 plasmid carrying the resistance gene for hygromycin with Cellfectin II (Life Technologies),
461 and the selection process was started 2 d after transfection by supplementing the media
462 with 250 µg/ml Hygromycin B.

463 SNAP quench chase pulse experiments

464 Cells overexpressing either SNAP-tagged CENP-A or CAL1 proteins were treated with dsRNA
465 as described in RNAi section. After 3 days, cells were collected and incubated in fresh SM
466 containing 10 µM SNAP-Cell Block (New England Biolabs S9106), for 30 min at 25 °C, 400
467 rpm. Cells were then pelleted, washed 3 times (1st wash for 30 min, at 25 °C, 400 rpm) and
468 plated in conditional medium. After 24 h, cells were collected and incubated with 4 µM
469 SNAP-Cell TMR-Star (New England Biolabs S9105) or SNAP-SiR647 (New England Biolabs
470 S9102) for 15 min at 25 °C, 400 rpm, protected from light. The cells were then pelleted,
471 washed 3 times with SM (1st wash for 30 min, at 25 °C, 400 rpm), one time in PBS and
472 prepared for imaging. Cells were settled on a glass coverslip for 10 min, fixed with 4 % PFA
473 for 10 min, washed three times in PBS, and counterstained with DAPI before mounting.

474 SNAP pulse-chase

475 Cells overexpressing either SNAP-tagged CENP-A or CAL1 proteins were treated with dsRNA
476 as described in RNAi section. After 3 days, cells were collected and incubated in fresh
477 medium containing 4 µM SNAP-Cell TMR-Star (New England Biolabs, Inc.) for 15 min at 25
478 °C, 400 rpm, protected from light. Cells were then washed 3 times with SM (1st wash for 30

479 min, at 25 °C, 400 rpm) and plated in conditional medium. After 24 h, cells were collected
480 and prepared for imaging as previously described.

481 SNAP live imaging

482 To follow incorporation of newly synthesized SNAP-CENP-A, SNAP-CENP-A was blocked as
483 previously described (see section SNAP quench chase pulse). Cells were then resuspended in
484 conditional medium containing 0.5 µM SNAP-640 dye (Butkevich et al., 2017) and placed
485 into an Ibidi imaging chamber before imaging.

486 **Immunofluorescence**

487 IF was essentially performed as described previously (Erhardt et al., 2008). Cells were
488 harvested, washed once with PBS and placed to settle on a glass coverslip for 10 min before
489 fixation with 4 % PFA for 10 min. Cells were washed three times in PBS and permeabilized
490 for 5 min with PBS containing with 0.5 % Triton X-100. Unspecific binding was prevented by
491 blocking the cells for 30 min with 1 % BSA in PBS. Primary antibodies diluted in blocking
492 solution were incubated for 30 min at RT. After three washes with PBS, cells were incubated
493 with the corresponding, fluorescently labeled secondary antibodies (diluted in blocking
494 solution) for 30 min at RT. The secondary antibody incubation and all the following steps
495 were performed while protected from light. After three washes in PBS, DNA was stained for
496 5 min with DAPI (1 µg/ml in PBS). The cells were then washed two more times with PBS
497 before mounting in Aqua/Polymount medium (Polysciences, Inc.) on a glass slide.

498 **Preparation of mitotic chromosome spreads**

499 Mitotic chromosome spreads were essentially performed as described previously (Mathew
500 et al., 2014). To obtain mitotic chromosomes, $2x10^5$ exponentially growing cells were
501 arrested in mitosis with 2.5 µg/µl Colcemid for 1 h, centrifuged for 3 min at 800 *g*,

502 resuspended in 0.5 ml hypotonic sodium citrate solution (0.5 % Na-citrate in ddH2O), and
503 incubated for 8–10 min. Cells were spun on positively charged slides in a cytocentrifuge
504 (Shandon 4 Cytospin; Thermo Fisher Scientific) at 900 rpm for 10 min. Mitotic chromosome
505 spreads were fixed with 4 % PFA for 10 min and subsequently treated for IF.

506 **Microscopy and Image analysis**

507 All Images were acquired on a DeltaVision Core system (Applied Precision) equipped with an
508 Olympus UPlanSApo 100X oil immersion objective (n.a. 1.4) at binning 1x1 (mitotic figures)
509 or 2x2 (interphase). If not stated otherwise, images were taken as z stacks of 0.3 µm
510 increments. All images were deconvolved (20 cycles additive with noise filtering) and
511 maximum-projected using the Applied Precisions soft-WoRx 3.7.1 suite. Image
512 quantification was done using ImageJ software. For determining the number and intensities
513 of centromeric dots of CAL1 and CENP-A, a set of plugins developed by the Nikon Imaging
514 Centre, University Heidelberg was used. After marking the nuclear boundaries in the DAPI
515 channel and saving them with the ROI tool, the spots in the channel of interest were
516 enhanced using the DoG spot enhancer plugin. The threshold was adjusted using ‘‘Li’’
517 instead of default settings. The number of spots with their mean intensities relative to the
518 nuclear area was determined using the ROI particle analyzer plugin.

519 Time-lapse imaging was performed on a DeltaVision Core system (Applied Precision)
520 equipped either with an Olympus 60X/1.42, N Plan Apo oil immersion objective or an
521 Olympus 40X/1.35, UApo/340 oil objective, at binning 2x2 with 3 min (mitosis duration and
522 fidelity measurements) or 15 min (SNAP-CENP-A live imaging) time-lapse series, for 16 h,
523 with z stacks of 1 µm increment.

524 FRAP was performed on a Zeiss LSM 780 confocal microscope equipped with a 63x/1.4 oil
525 immersion objective. Number of focal planes per time point, as well as time intervals and

526 total duration were adjusted according to experimental needs. The spacing of focal planes
527 was 1 µm in all experiments. Recovery of EGFP-CENP-A signal was analyzed using FRAP
528 analysis plugin developed by ZMBH imaging facility. After marking the boundaries of the cell
529 of interest, the threshold allowing visualization of centromeric signal exclusively was defined
530 on pre-bleach image. Total intensity of the thresholded signal was then measured for each
531 time point as well as the area. Similar measurements were performed on non-bleached cells
532 from the same area to determine the photobleaching level in each time-series. After
533 correction, EGFP-CENP-A signal intensity was plotted against the time, a linear regression
534 curve was fitted and the rate of recovery extracted.

535 **Immunoprecipitation**

536 GFP-tagged proteins were isolated using a GFP-specific single chain antibody (GBP) coupled
537 to NHS-activated Sepharose (GE) (Rothbauer et al., 2008). A total of 1.0–2.0 x 10^8 cells were
538 lysed in two pellet volumes of 20 mM Tris (pH 7.5), 1 % NP-40, 250 mM NaCl, 2 mM PMSF, 2
539 mg/ml aprotinin, 5 mg/ml leupeptin, 1 mg/ml pepstatin and Roche anti-proteases cocktail
540 tablet for 15 min at 4 °C. After clearing the lysate by centrifugation, the supernatant was
541 incubated for 2 h at 4 °C with 50 µl pre-equilibated GBP-beads. The beads were washed six
542 times with lysis buffer and eluted with 2x Laemmli buffer 5 min at 95 °C.

543 **Antibodies**

544 The following primary antibodies were used: rabbit H3 (Abcam AB 1791), rabbit CAL1 (Bade
545 et al., 2014), chicken CENP-A (from Dr. Heun), rabbit CENP-A (Active Motif 39713), rabbit
546 YFP (from Pr. Bukau), mouse tubulin (Sigma T9026), mouse V5 (Invitrogen V8012), sheep
547 Scp105R (from Dr. Glover), rabbit Zw10 (from Dr. Goldberg), guinea pig CENP-C (Erhardt et
548 al., 2008), rabbit phospho-S10 histone H3 (Abcam ab5176), BubR1 (from Dr. Glover).

549 Secondary antibodies coupled to Alexa Fluor 488, Alexa Fluor 546 and Alexa Fluor 647
550 fluorophores (Molecular Probes) were used for IF, and horseradish peroxidase-conjugated
551 secondary antibodies (Sigma) were used for WB analysis.

552 **Reverse transcription and Quantitative qPCR**

553 RNA was isolated using Trizol(R) according to the manufacturer's procedures. Whole
554 genome cDNA synthesis was performed using the Quantitect Reverse Transcription kit
555 (Invitrogen), with a combination of oligo (dT) and random hexamer primers in equal
556 proportions. A control reaction with no reverse transcription was always performed in
557 parallel.

558 qPCR was performed after cDNA synthesis on a LightCycler 480 (Roche) using LightCycler
559 480 SYBR Green I Master (Roche). All reactions were run in triplicate in a LightCycler 480
560 multiwell plate. Actin was used as a reference. The level of each targeted gene in the control
561 mock-treated sample was normalized to 1, and compared with the corresponding–depleted
562 samples.

563

564 **Yeast two hybrid**

565 Protein-protein interactions were tested using pMM5 and pMM6 fusion constructs and the
566 yeast strain SGY37VIII. The YTH was performed as described previously (Schramm et al.,
567 2000). In short, interactions were judged based on the activity of β-galactosidase that
568 results in the conversion of X-Gal (5-bromo-4-chloro-3-indolyl-b-D-galactosidase) into a blue
569 dye.

570

571 **Acknowledgements:**

572 We thank B. Bukau, D. Glover, M. Przewloka, M. Goldberg, R. Karess for antibodies and
573 constructs, V. Belov, A. Butkevich and the Facility of synthetic chemistry of the Max Planck
574 Institute for Biophysical Chemistry (MPIBPC) for the gift of the compound 640SiRH-BG. We
575 thank the ZMBH Imaging Facility and A. Jafar Pour for ImageJ FRAP analysis plugins; H.
576 Lorenz for help with imaging, R. Vlijm and the Erhardt laboratory members for discussions;
577 E. Schiebel and S. Corless for critical comments on the manuscript. We acknowledge funding
578 from the Deutsche Forschungsgemeinschaft through the grant EXC81 (CellNetworks),
579 ER576/2-2, SFB1036, the European Research Council through the grant ERC-CoG-682496
580 (cenRNA) to SE. ALP is an alumna of the CellNetworks postdoc program.

581

582 Competing interests: No competing interests declared

583

584

585 **Figures legends**

586 **Figure 1: RZZ recruitment to kinetochores does not require Spc105R in *Drosophila*.**

587 **A.** Immunofluorescence of cells expressing GFP-Rod, GFP-Zw10 or GFP-Zwilch in
588 combination with mCherry-Tubulin after depletion of RZZ components as indicated. After 96
589 h dsRNA treatment, cells were fixed and stained with anti-GFP antibody (green) and anti-
590 CENP-A (red), DNA was counterstained with DAPI. **B.** ***Upper panel.*** Prometaphase cells from
591 A. were counted for the presence or absence of GFP signal at kinetochores. ***Lower panel.***
592 Quantification of A. showing the total GFP-RZZ kinetochore intensity per cell. GFP
593 fluorescence intensity at kinetochores was measured for each cell and then normalized
594 within one experiment allowing pooling of the measurements for at least 3 experiments per
595 condition. **C.** Immunofluorescence of GFP-Zw10/mCherry-Tubulin expressing cells after
596 depletion of Spc105R. At day 4 of RNAi, cells were fixed and stained with anti-GFP (green)
597 and anti-Spc105R antibodies (red), DNA was counterstained with DAPI. **D.** Quantifications
598 of C. ***Left.*** Prometaphase cells were counted for the presence or absence of GFP-Zw10 signal
599 at kinetochores. ***Right.*** Total GFP-Zw10 kinetochore intensity per cell measured as in B. **E.**
600 Immunofluorescence of GFP-Zw10/mCherry-Tubulin expressing cells after depletion of
601 Mis12. After 96 h dsRNA treatment, cells were fixed and stained with anti-GFP (green) and
602 anti-Spc105R (red) antibodies, DNA was counterstained with DAPI. **F.** Quantifications of E.
603 ***Left.*** Prometaphase cells were counted for the presence or absence of GFP-Zw10 signal at
604 kinetochores. ***Right.*** Total GFP-Zw10 kinetochore intensity per cell measured as in B. All
605 graphs show Mean +/- SEM of 3 experiments (n>90 cells), Student t-test (n.s.: non-
606 significant; *: $p<0.05$; **: $p<0.01$; ***: $p<0.001$). Scale bar= 2 µm.

607

608 **Figure 2: RZZ recruitment to the kinetochore depends on a direct interaction with inner**
609 **centromere proteins.**

610 **A.** Immunofluorescence of GFP-Zw10/mCherry-Tubulin expressing cells after depletion of
611 CENP-A. At day 4 of RNAi, cells were fixed and stained with anti-GFP (green), anti-CENP-A
612 (red) antibodies, DNA was counterstained with DAPI. Scale bar= 2 µm. **B.** Quantifications of
613 A. ***Left.*** Prometaphase cells were counted for the presence or absence of GFP-Zw10 signal at
614 kinetochores. ***Right.*** Total GFP-Zw10 kinetochore intensity was measured in each cell,
615 normalized and plotted. Mean +/- SEM of 3 experiments (n>90 cells), Student t-test (*:
616 $p<0.05$; ***: $p<0.001$). **C.** Co-immunoprecipitation of RZZ components with centromeric
617 proteins. GFP (Ctrl), GFP-Rod, GFP-Zw10, GFP-Zwilch and GFP-RINT1 proteins were
618 immunoprecipitated using the GFP-binding protein (GBP). Pulled down fractions were
619 analyzed by immunoblotting for the presence of CAL1, CENP-A and Zw10. **D.** Yeast two
620 hybrid interaction tests using the RZZ components Zw10, Zwilch and three domains of ROD
621 with CAL1 and CENP-A. Blue color reflects the interaction between the 2 proteins tested.

622

623 **Figure 3: Zw10 affects the loading of CENP-A during mitosis.**

624 **A.** Time line of RNAi experiment followed by a Quench-Chase-Pulse SNAP-tag experiment.
625 After 72 h dsRNA treatment, cells were incubated with SNAP-Block to quench existing SNAP-
626 CENP-A molecules (Q), washed and cultured for 24 h. After 24 h chase, cells were incubated
627 with TMR-Star (red) to stain newly synthesized SNAP-CENP-A molecules (P). The images
628 show representative immunofluorescence staining of SNAP-CENP-A expressing cells after
629 Zw10 or control depletion. DNA was counterstained with DAPI. Scale bar= 2 µm. **B.**
630 Quantification of A. showing the total SNAP-CENP-A centromeric intensity per nucleus as %

631 of control. Mean +/- SEM of 3 experiments (n>300 cells), Student t-test (***: p<0.001). **C.**
632 FRAP of GFP-CENP-A in mitosis after Zw10 depletion. After 72 h dsRNA treatment, GFP-
633 CENP-A signal was partially (about 50-60 %) bleached in prophase and cells were imaged
634 until telophase. Time lapse: 90 s. Scale bar= 2 µm. **D.** Quantification of C. The total GFP-
635 CENP-A centromeric signal of the cells shown in C is displayed. **E.** Recovery rate of GFP-
636 CENP-A in control and Zw10-depleted cells. Mean +/- SEM, n≥10 cells, Student t-test (n.s=
637 non-significant).

638

639 **Figure 4: CENP-A loading is correlated with mitosis duration.**

640 **A.** Time-lapse imaging of H2B-GFP/mCherry-tubulin expressing cells after Zw10 depletion.
641 After 72 h dsRNA treatment, cells were imaged for 16 h. Time lapse 3 min. Scale bar= 2 µm.
642 **B.** Quantification of A. The mitosis duration from nuclear envelope breakdown (determined
643 by mCherry-Tubulin nuclear diffusion concomitant to DNA condensation) to anaphase entry
644 is shown. Mean +/- SEM, n>200 cells. Student t-test (***: p<0.001). **C.** SNAP-CENP-A
645 incorporation in BubR1, Mad2, Mis12, Spindly or Cdc27 depleted cells. After 72 h dsRNA
646 treatment, a Quench-Chase-Pulse experiment (scheme in Fig. 3A) was performed to stain
647 newly synthesized SNAP-CENP-A molecules. DNA was counterstained with DAPI. Scale bar: 2
648 µm. **D.** Quantification of C. The total SNAP-CENP-A centromeric signal intensity per nucleus
649 is shown as % of control dsRNA-treated cells. Mean +/- SEM of 3 experiments (n>300 cells),
650 Student t-test (*n.s.*: non-significant; ***: p<0.001). **E.** The recovery rate of GFP-CENP-A after
651 photobleaching in mitosis is plotted against the mitosis duration for each analyzed cell.
652 Pearson's correlation test, p<0.01.

653

654 **Figure 5: CENP-A levels affects mitosis duration.**

655 **A.** Immunoblot showing CENP-A knockdown efficiency in GFP-CENP-A/mCherry-Tubulin
656 expressing cells. An anti-CENP-A antibody was used to detect endogenous CENP-A and
657 overexpressed GFP-CENP-A. **B.** Time-lapse imaging of GFP-CENP-A/mCherry-tubulin
658 expressing cells after CENP-A depletion. After 72 h dsRNA treatment, cells were imaged for
659 16 h. Time lapse 3 min. Scale bar= 5 µm. **C.** Quantification of B. showing the mitosis duration
660 of control and CENP-A depleted cells. Mean +/- SEM, n>80 cells. Student t-test (***:
661 p<0.001). **D.** Immunoblot showing CENP-A levels in the different cell lines used. CENP-A
662 antibody detects endogenous and tagged versions of CENP-A. GFP-CENP-A and SNAP-CENP-
663 A are under the constitutive *copia* promoter. CENP-A-GFP expression can be induced by
664 activating the *metallothionein* promoter with $CuSO_4$. H3 serves as loading control. **E.**
665 Immunofluorescence of CENP-A-GFP cells. CENP-A-GFP expression was induced with 10 µM
666 $CuSO_4$ for 2 h. Cells were washed and cultured in conditional medium for 22 h before
667 fixation. DNA was counterstained with DAPI. Scale bar= 2 µm. **F.** Quantification of E.
668 showing the total CENP-A-GFP centromeric intensity per nucleus as % of control. Mean +/-
669 SEM of 3 experiments (n>300 cells), Student t-test (n.s= non-significant). **G.** Time lapse
670 imaging of cells expressing mCherry-tubulin and inducible CENP-A-GFP. GFP-CENP-A
671 expression was induced by addition of 10 µM $CuSO_4$ to the medium for 2 h. Cells were
672 washed before imaging (16 h). Time lapse 3 min. Scale bar= 5 µm. The intensity levels of
673 CENP-A-GFP in control cells are shown enhanced for visualization purposes **H.** Quantification
674 of G. showing mitosis duration of control and CENP-A-GFP expressing cells. Mean +/- SEM,
675 n>300 cells. Student t-test (***: p<0.001). **I.** Mitotic phenotypes of CENP-A-GFP/mCherry-
676 Tubulin cells imaged in G. Cells were scored for the accuracy of mitosis: normal or defective

677 (presence of lagging chromosomes in anaphase, formation of tripolar spindles). Mean +/-
678 SEM n > 200 cells. Student t-test (n.s.: non-significant).

679

680 **Figure 6: CAL1 overexpression leads to increased CENP-A levels at centromeres.**

681 **A.** Immunoblot of CENP-A (either GFP or SNAP N-terminally tagged) expressing cells with or
682 without concomitant CAL1 overexpression. CAL1-V5 expression was induced by addition of
683 100 µM $CuSO_4$ for 24 h. Anti-CAL1 (endogenous CAL1 and CAL1-V5), anti-CENP-A
684 (endogenous CENP-A and tagged-CENP-A) and anti-H3 antibodies were used. **B.**
685 Immunofluorescence of CAL1-V5/GFP-CENP-A expressing cells. CAL1-V5 expression was
686 induced as in A. Cells were fixed and stained with anti-V5 antibody (red). DNA was
687 counterstained with DAPI. **C.** Metaphase chromosomes of CAL1-V5 expressing cells. CAL1-V5
688 expression was induced as in A. Metaphase chromosomes were prepared and stained with
689 anti-CENP-A antibody. DNA was counterstained with DAPI. **D.** Quantification of B. GFP-
690 CENP-A signal intensity per centromere was measured and is shown as % of non-induced
691 control cells. **E.** Immunofluorescence of CAL1-V5/GFP-CENP-A expressing cells. CAL1-V5
692 expression was induced as in A. Then the cells were fixed and stained with anti-CENP-C
693 antibody (red). DNA was counterstained with DAPI. **F.** Quantification of E. CENP-C signal
694 intensity per centromere was measured and is shown as % of non-induced control cells. **G.**
695 Immunofluorescence of newly synthesized SNAP-CENP-A in CAL1 overexpressing cells. CAL1-
696 V5 expression was induced as in A. SNAP-CENP-A molecules were quenched with SNAP-
697 Block. A 24 h chase was performed in presence of $CuSO_4$, before labeling with SNAP-SiR647
698 and fixation. DNA was counterstained with DAPI. **H.** Quantification of G. SNAP-CENP-A signal
699 intensity per centromere was measured and is shown as % of non-induced control. All

700 graphs show Mean +/- SEM of 3 experiments (n>300 cells), Student t-test (n.s.: non-
701 significant; *: p<0.05; **: p<0.01). Scale bar= 2 µm.

702

703 **Figure 7: Overexpression of CAL1 leads to CENP-A centromeric loading outside of mitosis.**

704 **A.** Time-lapse imaging of H2B-GFP/mCherry Tubulin cells with or without concomitant
705 overexpression of CAL1. CAL1-V5 expression was induced for 24 h. The cells were imaged for
706 16 h. Time lapse 3 min. Scale bar= 2 µm. **B.** Quantification of A showing the mitosis duration.
707 Mean +/- SEM, n > 200 cells. Student t-test (***: p<0.001). **C.** FRAP experiments of GFP-
708 CENP-A in mitosis in CAL1-overexpressing cells. CAL1-V5 expression was induced for 24 h.
709 GFP-CENP-A signal was partially bleached in prophase and cells were imaged until
710 telophase. Time lapse: 90 s. Scale bar= 2 µm. **D.** Recovery rate of GFP-CENP-A in control and
711 CAL1-overexpressing cells. Mean +/- SEM, n≥ 12 cells, Student t-test (*: p<0.05; **: p<0.01).
712 **E.** Time-lapse imaging of SNAP-CENP-A/mCherry-Tubulin cells with or without concomitant
713 overexpression of CAL1. CAL1-V5 expression was induced for 24 h. Then the cells were
714 incubated with SNAP-Block to quench existing SNAP-CENP-A molecules, washed and
715 resuspended in conditional medium containing 0.5 µM SNAP-640 dye. Cells were imaged for
716 16 h to visualize newly synthesized SNAP-CENP-A. Time lapse 15 min. Scale bar= 2 µm.
717 Intensity levels have been adjusted separately for each condition. **F-G.** Quantifications of E.
718 **F.** Table showing the % of SNAP-CENP-A positive cells (+ cells) and the timing of loading. **G.**
719 For each cycling cell, the earliest detection time point of SNAP-CENP-A (Y-axis) is plotted
720 versus the time of cytokinesis (X-axis). t0 on both axis corresponds to start of imaging after
721 SNAP-Block.

722

723 Online supplemental materials include 6 figures and 10 videos. Fig. S1 shows localization of
724 the GFP-tagged RZZ-proteins during cell cycle, qPCR and WB results for RNAi efficiency. Fig.
725 S2 shows Spc105R localization in Zw10-depleted cells, Zw10 localization in CAL1-depleted
726 cells, localization of GFP-RINT during cell cycle and yeast two hybrid with CAL1 and Zw10
727 fragments. Fig. S3 shows SNAP-CAL1 quench-chase-pulse experiment in Zw10-depleted
728 cells, centromeric SNAP-CENP-A stability assay and GFP-CENP-A FRAP in early G1. Fig. S4
729 shows qPCR results for RNAi efficiency, SNAP-CENP-A and SNAP-CAL1 quench-chase-pulse
730 experiments in different RNAi and drug treatment. Fig. S5 shows SAC activity and
731 kinetochore components recruitment in CAL1-overexpressing cells. Fig. S6 shows SNAP-
732 CENP-A centromeric loading outside mitosis.

733

734 **Supplemental figures legends**

735 **Figure S1 related to fig. 1.**

736 Localization of GFP-ROD (**A.**), GFP-Zwilch (**B**.), GFP-Zw10 (**C**.) during cell cycle. Cells
737 expressing each GFP-RZZ component concomitant with mCherry-Tubulin were fixed and
738 stained with anti-GFP (green) and anti-CENP-A (red) antibodies, DNA was counterstained
739 with DAPI. Scale bar= 2 µm. **D**. qPCR results showing mRNA levels after indicated
740 knockdown in percent of control. **E.** Immunoblot showing protein levels after dsRNA
741 treatment.

742 **Figure S2 related to fig. 1-2.**

743 **A.** Immunofluorescence of S2 cells after depletion of Zw10. At day 4 of RNAi, cells were fixed
744 and stained with anti-Zw10 (green), anti-Spc105R (red) and anti-tubulin (grey) antibodies,

745 DNA was counterstained with DAPI. Scale bar= 2 µm. **B.** Quantification of A. Prometaphase
746 cells were counted for the presence or absence of Spc105R signal at kinetochores. **C.**
747 Immunofluorescence of GFP-Zw10/mCherry-Tubulin expressing cells after depletion of
748 CAL1. After 96 h dsRNA treatment, cells were fixed and stained with anti-GFP (green) and
749 anti-CENP-A (red) antibodies, DNA was counterstained with DAPI. Scale bar= 2 µm. **D.**
750 Localization of GFP-RINT1, during cell cycle. Cells expressing each GFP-RINT1 concomitant
751 with mCherry-Tubulin were fixed and stained with anti-GFP (green) and anti-CENP-A (red)
752 antibodies, DNA was counterstained with DAPI. Scale bar= 2 µm. **F.** Yeast two hybrid
753 interaction tests. Blue color reflects the interaction between the 2 proteins tested. **G.**
754 Scheme showing CAL1 functional domains and its binding to its known partners. BD: binding
755 domain.

756

757 **Figure S3 related to fig. 3**

758 **A.** Immunofluorescence of SNAP-CAL1 expressing cells after Zw10 depletion. After 72 h
759 dsRNA treatment, a Quench-Chase-Pulse experiment (scheme in Fig. 3A) was performed to
760 stain newly synthesized SNAP-CAL1 molecules. DNA was counterstained with DAPI. Scale
761 bar= 2 µm. **B.** Quantification of A. showing the total SNAP-CAL1 centromeric intensity per
762 nucleus as % of control. Mean +/- SEM of 3 experiments (n>300 cells), Student t-test (**:
763 p<0.01). **C.** Immunofluorescence of SNAP-CENP-A expressing cells after Zw10 depletion.
764 After 72 h dsRNA treatment, cells were incubated with TMR-Star (P) to stain existing SNAP-
765 CENP-A molecules, washed and put back in culture (t0). After 24 h chase, cells were fixed
766 (t24). Note that no SNAP-Block was performed for this experiment. DNA was counterstained
767 with DAPI. Scale bar= 2 µm. **D.** Quantification of C. showing the total SNAP-CENP-A

768 centromeric intensity per nucleus as % of t0. Mean +/- SEM of 3 experiments (n>300 cells),
769 Student t-test (n.s= non-significant). **E.** FRAP of GFP-CENP-A in G1 phase. Cells expressing
770 GFP-CENP-A and mCherry-Tubulin were followed through mitosis, GFP-CENP-A signal was
771 partially bleached in early G1 and cells were further imaged for > 2 h. Time lapse: 6 min.
772 Scale bar: 2 µm. **F.** Quantification of E. The total GFP-CENP-A centromeric signal of 4
773 representative cells is shown.

774

775 **Figure S4 related to fig. 4**

776 **A.** qPCR results showing mRNA levels after indicated knockdown in SNAP-CENP-A cells as
777 percent of control. **B.** Immunofluorescence of SNAP-CENP-A expressing cells after MG132 or
778 Nocodazole treatment. A Quench-Chase-Pulse experiment was performed to stain newly
779 synthesized SNAP-CENP-A molecules. The 24 h chase was performed in presence or absence
780 of the indicated drug. Cells were stained with an anti-S10-phospho-H3 antibody to identify
781 mitotic cells. DNA was counterstained with DAPI. Scale bar= 2 µm. **C.** Quantification of B.
782 showing the SNAP-CENP-A centromeric intensity as % of control. Only Phospho-H3 positive
783 cells were analyzed. Mean+/- SEM of 3 experiments (n>300 cells), Student t-test (n.s= non-
784 significant). **D.** Quantification showing the total SNAP-CAL1 centromeric intensity per
785 nucleus as % of control after depletion of the indicated proteins. Mean+/- SEM of 3
786 experiments (n>300 cells), Student t-test (**: p<0.01; n.s.: non-significant).

787

788 **Figure S5 related to fig. 7**

789 **A.** Mitotic phenotypes of H2B-GFP/mCherry-Tubulin expressing cells with or without
790 concomitant overexpression of CAL1. CAL1-V5 expression was induced for 24 h with 100 µM
791 $CuSO_4$ then the cells were imaged for 16 h. Cells were scored for the accuracy of mitosis:
792 normal or defective (presence of lagging chromosomes in anaphase, formation of tripolar
793 spindles). Mean +/- SEM n > 200 cells. Student t-test (n.s.: non-significant). **B.** Amount of
794 kinetochore proteins recruited during mitosis in presence or absence of CAL1
795 overexpression. CAL1-V5 expression was induced for 24 h in GFP-CENP-A/mCherry-Tubulin
796 cells. Cells were then fixed and stained with anti-CENP-C (upper panel, red), anti-Spc105R
797 (middle panel, red) or anti-BubR1 antibody (lower panel, red). DNA was counterstained with
798 DAPI. Scale bar= 2 µm. Kinetochore signal intensity of the indicated proteins is shown as %
799 of control. Only prometaphase cells were analyzed. Mean +/- SEM of 3 experiments (n > 300
800 cells). Student t-test (n.s.: non-significant). **C.** Stills from time-lapse imaging experiments
801 showing GFP-CENP-A/mCherry-Tubulin cells with or without CAL1 overexpression imaged
802 immediately after addition of 1 µM Taxol and after 5 h. CAL1-V5 expression was induced for
803 24 h. Then 1 µM taxol was added and the cells were imaged for 16 h. **D.** Quantification of C.
804 showing the percentage of cells that arrest (arrest) in response to Taxol treatment or arrest
805 and restart (finish).

806

807 **Figure S6 related to fig. 7**

808 **A.** Quantification of cells showing SNAP-CENP-A signal at centromeres in control and CAL1-
809 overexpressing cells after 4 h MG132 treatment. CAL1-V5 expression was induced for 24 h.
810 then the cells were incubated for 2 h with MG132 to arrest cells in mitosis prior to SNAP-
811 CENP-A block. A 4-h chase was performed in presence of MG132 to allow synthesis and

812 incorporation of new SNAP-CENP-A into centromeres before incubation with SNAP-Si647
813 and fixation. **B.** Immunofluorescence of SNAP-CENP-A in control and CAL1 overexpressing
814 cells. CAL1-V5 expression was induced for 24 h. The cells were then incubated with SNAP-
815 Block, washed and resuspended in conditional medium containing SNAP-640 dye. After 20
816 h, the cells were washed 3 times before fixation and immunostaining with an anti-CENP-A
817 antibody (green). Cells were also taken after block, stained with 0.5 µM SNAP-640 dye for 15
818 min to check the efficiency of the block. DNA was counterstained with DAPI. Scale bar= 2
819 µm. **C.** Quantification of B. showing the percentage of cells positive for centromeric SNAP-
820 CENP-A staining. **D.** Quantification of B. showing the total SNAP-CENP-A centromeric
821 intensity per nucleus as % of control. All graphs show Mean +/- SEM of 3 experiments
822 (n>300 cells), Student t-test (n.s.: non-significant; *: $p<0.05$; **: $p<0.01$).

823

824 **Supplemental Videos.**

825 **Video 1 (related to Figure 4A).**

826 H2B-GFP/mCherry-tubulin expressing cells after Ctrl dsRNA treatment (72 h). Imaging was
827 performed for 16 h on a Deltavision microscope (60X, Bin 2), at 25 °C. Time lapse 3 min.
828 Scale bar= 5 µm.

829 **Video 2 (related to Figure 4A):**

830 H2B-GFP/mCherry-tubulin expressing cells after Zw10 dsRNA treatment (72 h). Imaging was
831 performed for 16 h on a Deltavision microscope (60X, Bin 2), at 25 °C. Time lapse 3 min.
832 Scale bar= 5 µm.

833 **Video 3 (related to Figure 5B):**

834 GFP-CENP-A/mCherry-Tubulin expressing cells after Ctrl dsRNA treatment (72 h). Imaging
835 was performed for 16 h on a Deltavision microscope (40X, Bin 2), at 25 °C. Time lapse 3 min.
836 Scale bar= 5 µm.

837 **Video 4 (related to Figure 5B):**

838 GFP-CENP-A/mCherry-Tubulin expressing cells after CENP-A dsRNA treatment (72 h).
839 Imaging was performed for 16 h on a Deltavision microscope (40X, Bin 2), at 25 °C. Time
840 lapse 3 min. Scale bar= 5 µm.

841 **Video 5 (related to Figure 5G):**

842 CENP-A-GFP/mCherry-tubulin expressing cells. Visible CENP-A-GFP results from leaky
843 metallothionein promoter. Imaging was performed for 16 h on a Deltavision microscope
844 (40X, Bin 2), at 25 °C. Time lapse 3 min. Scale bar= 5 µm.

845 **Video 6 (related to Figure 5G):**

846 CENP-A-GFP/mCherry-tubulin expressing cells. CENP-A-GFP expression was induced for 2 h
847 with 10 µM $CuSO_4$ then washed 3 times before being placed in Ibidi chamber. Imaging was
848 performed for 16 h on a Deltavision microscope (40X, Bin 2), at 25 °C. Time lapse 3 min.
849 Scale bar= 5 µm.

850 **Video 7 (related to Figure 7A):**

851 H2B-GFP/mCherry-tubulin expressing cells containing inducible CAL1-V5. No CAL1-V5
852 induction. Imaging was performed for 16 h on a Deltavision microscope (60X, Bin 2), at 25
853 °C. Time lapse 3 min. Scale bar= 5 µm.

854 **Video 8 (related to Figure 7A):**

855 H2B-GFP/mCherry-tubulin expressing cells containing inducible CAL1-V5. CAL1-V5
856 expression was induced for 24 h prior to imaging with 100 µM $CuSO_4$. Imaging was

857 performed for 16 h on a Deltavision microscope (60X, Bin 2), at 25 °C. Time lapse 3 min.
858 Scale bar= 5 µm.

859 **Video 9 (related to Figure 7E):**

860 SNAP-CENP-A/mCherry-tubulin expressing cells containing inducible CAL1-V5. No CAL1-V5
861 induction. SNAP-CENP-A molecules were quenched before addition of 0.5 µM SNAP-640
862 dye. Imaging was performed for 16 h on a Deltavision microscope (60X, Bin 2), at 25 °C.
863 Time lapse 15 min. Scale bar= 5 µm.

864 **Video 10 (related Figure 7E):**

865 SNAP-CENP-A/mCherry-tubulin expressing cells containing inducible CAL1-V5. CAL1-V5
866 expression was induced for 24 h with 100 µM $CuSO_4$. SNAP-CENP-A molecules were
867 quenched before addition of 0.5 µM SNAP-640 dye. Imaging was performed for 16 h on a
868 Deltavision microscope (60X, Bin 2), at 25 °C. Time lapse 15 min. Scale bar= 5 µm.

869

870 **References**

871 Ahmad, K., and S. Henikoff. 2001. Centromeres are specialized replication domains in
872 heterochromatin. *J Cell Biol*. 153:101-110.
873 Bade, D., A.L. Pauleau, A. Wendler, and S. Erhardt. 2014. The E3 ligase CUL3/RDX controls
874 centromere maintenance by ubiquitylating and stabilizing CENP-A in a CAL1-dependent manner. *Dev*
875 *Cell*. 28:508-519.
876 Barisic, M., and S. Geley. 2011. Spindly switch controls anaphase: spindly and RZZ functions in
877 chromosome attachment and mitotic checkpoint control. *Cell Cycle*. 10:449-456.
878 Basto, R., R. Gomes, and R.E. Karess. 2000. Rough deal and Zw10 are required for the metaphase
879 checkpoint in Drosophila. *Nat Cell Biol*. 2:939-943.
880 Basto, R., F. Scaerou, S. Mische, E. Wojcik, C. Lefebvre, R. Gomes, T. Hays, and R. Karess. 2004. In
881 vivo dynamics of the rough deal checkpoint protein during Drosophila mitosis. *Curr Biol*. 14:56-61.
882 Basu, J., E. Logarinho, S. Herrmann, H. Bousbaa, Z. Li, G.K. Chan, T.J. Yen, C.E. Sunkel, and M.L.
883 Goldberg. 1998. Localization of the Drosophila checkpoint control protein Bub3 to the kinetochore
884 requires Bub1 but not Zw10 or Rod. *Chromosoma*. 107:376-385.
885 Blower, M.D., T. Daigle, T. Kaufman, and G.H. Karpen. 2006. Drosophila CENP-A mutations cause a
886 BubR1-dependent early mitotic delay without normal localization of kinetochore components. *PLoS*
887 *Genet*. 2:e110.
888 Blower, M.D., and G.H. Karpen. 2001. The role of Drosophila CID in kinetochore formation, cell-cycle
889 progression and heterochromatin interactions. *Nat Cell Biol*. 3:730-739.

890 Buffin, E., D. Emre, and R.E. Karess. 2007. Flies without a spindle checkpoint. *Nat Cell Biol*. 9:565-572.
891 Buffin, E., C. Lefebvre, J. Huang, M.E. Gagou, and R.E. Karess. 2005. Recruitment of Mad2 to the
892 kinetochore requires the Rod/Zw10 complex. *Curr Biol*. 15:856-861.
893 Butkevich, A.N., V.N. Belov, K. Kolmakov, V.V. Sokolov, H. Shojaei, S.C. Sidenstein, D. Kamin, J.
894 Matthias, R. Vlijm, J. Engelhardt, and S.W. Hell. 2017. Hydroxylated Fluorescent Dyes for Live-Cell
895 Labeling: Synthesis, Spectra and Super-Resolution STED. *Chemistry*. 23:12114-12119.
896 Caldas, G.V., T.R. Lynch, R. Anderson, S. Afreen, D. Varma, and J.G. DeLuca. 2015. The RZZ complex
897 requires the N-terminus of KNL1 to mediate optimal Mad1 kinetochore localization in human cells.
898 *Open Biol*. 5.
899 Chen, C.C., M.L. Dechassa, E. Bettini, M.B. Ledoux, C. Belisario, P. Heun, K. Luger, and B.G. Mellone.
900 2014. CAL1 is the Drosophila CENP-A assembly factor. *J Cell Biol*. 204:313-329.
901 Defachelles, L., S.G. Hainline, A. Menant, L.A. Lee, and R.E. Karess. 2015a. A maternal effect rough
902 deal mutation suggests that multiple pathways regulate Drosophila RZZ kinetochore recruitment. *J*
903 *Cell Sci*. 128:2952.
904 Defachelles, L., N. Raich, R. Terracol, X. Baudin, B. Williams, M. Goldberg, and R.E. Karess. 2015b. RZZ
905 and Mad1 dynamics in Drosophila mitosis. *Chromosome Res*. 23:333-342.
906 Emre, D., R. Terracol, A. Poncet, Z. Rahmani, and R.E. Karess. 2011. A mitotic role for Mad1 beyond
907 the spindle checkpoint. *J Cell Sci*. 124:1664-1671.
908 Erhardt, S., B.G. Mellone, C.M. Betts, W. Zhang, G.H. Karpen, and A.F. Straight. 2008. Genome-wide
909 analysis reveals a cell cycle-dependent mechanism controlling centromere propagation. *J Cell Biol*.
910 183:805-818.
911 Feijao, T., O. Afonso, A.F. Maia, and C.E. Sunkel. 2013. Stability of kinetochore-microtubule
912 attachment and the role of different KMN network components in Drosophila. *Cytoskeleton*
913 *(Hoboken)*. 70:661-675.
914 Gassmann, R., A. Essex, J.S. Hu, P.S. Maddox, F. Motegi, A. Sugimoto, S.M. O'Rourke, B. Bowerman, I.
915 McLeod, J.R. Yates, 3rd, K. Oegema, I.M. Cheeseman, and A. Desai. 2008. A new mechanism
916 controlling kinetochore-microtubule interactions revealed by comparison of two dynein-targeting
917 components: SPDL-1 and the Rod/Zwilch/Zw10 complex. *Genes Dev*. 22:2385-2399.
918 Griffis, E.R., N. Stuurman, and R.D. Vale. 2007. Spindly, a novel protein essential for silencing the
919 spindle assembly checkpoint, recruits dynein to the kinetochore. *J Cell Biol*. 177:1005-1015.
920 Heun, P., S. Erhardt, M.D. Blower, S. Weiss, A.D. Skora, and G.H. Karpen. 2006. Mislocalization of the
921 Drosophila centromere-specific histone CID promotes formation of functional ectopic kinetochores.
922 *Dev Cell*. 10:303-315.
923 Huang, J.Y., and J.W. Raff. 2002. The dynamic localisation of the Drosophila APC/C: evidence for the
924 existence of multiple complexes that perform distinct functions and are differentially localised. *J Cell*
925 *Sci*. 115:2847-2856.
926 Jansen, L.E., B.E. Black, D.R. Foltz, and D.W. Cleveland. 2007. Propagation of centromeric chromatin
927 requires exit from mitosis. *J Cell Biol*. 176:795-805.
928 Joglekar, A.P., and A.A. Kukreja. 2017. How Kinetochore Architecture Shapes the Mechanisms of Its
929 Function. *Curr Biol*. 27:R816-R824.
930 Kapanidou, M., N.L. Curtis, and V.M. Bolanos-Garcia. 2017. Cdc20: At the Crossroads between
931 Chromosome Segregation and Mitotic Exit. *Trends Biochem Sci*. 42:193-205.
932 Karess, R. 2005. Rod-Zw10-Zwilch: a key player in the spindle checkpoint. *Trends Cell Biol*. 15:386-
933 392.
934 Karess, R.E., and D.M. Glover. 1989. rough deal: a gene required for proper mitotic segregation in
935 Drosophila. *J Cell Biol*. 109:2951-2961.
936 Kasuboski, J.M., J.R. Bader, P.S. Vaughan, S.B. Tauhata, M. Winding, M.A. Morrissey, M.V. Joyce, W.
937 Boggess, L. Vos, G.K. Chan, E.H. Hinchcliffe, and K.T. Vaughan. 2011. Zwint-1 is a novel Aurora B
938 substrate required for the assembly of a dynein-binding platform on kinetochores. *Mol Biol Cell*.
939 22:3318-3330.

940 Kops, G.J., Y. Kim, B.A. Weaver, Y. Mao, I. McLeod, J.R. Yates, 3rd, M. Tagaya, and D.W. Cleveland.
941 2005. ZW10 links mitotic checkpoint signaling to the structural kinetochore. *J Cell Biol*. 169:49-60.
942 Li, J., N. Dang, D.J. Wood, and J.Y. Huang. 2017. The kinetochore-dependent and -independent
943 formation of the CDC20-MAD2 complex and its functions in HeLa cells. *Sci Rep*. 7:41072.
944 Lidsky, P.V., F. Sprenger, and C.F. Lehner. 2013. Distinct modes of centromere protein dynamics
945 during cell cycle progression in Drosophila S2R+ cells. *J Cell Sci*. 126:4782-4793.
946 Lince-Faria, M., S. Maffini, B. Orr, Y. Ding, F. Claudia, C.E. Sunkel, A. Tavares, J. Johansen, K.M.
947 Johansen, and H. Maiato. 2009. Spatiotemporal control of mitosis by the conserved spindle matrix
948 protein Megator. *J Cell Biol*. 184:647-657.
949 London, N., and S. Biggins. 2014. Mad1 kinetochore recruitment by Mps1-mediated phosphorylation
950 of Bub1 signals the spindle checkpoint. *Genes Dev*. 28:140-152.
951 Mathew, V., A.L. Pauleau, N. Steffen, A. Bergner, P.B. Becker, and S. Erhardt. 2014. The histone-fold
952 protein CHRAC14 influences chromatin composition in response to DNA damage. *Cell Rep*. 7:321-
953 330.
954 Mellone, B.G., K.J. Grive, V. Shteyn, S.R. Bowers, I. Oderberg, and G.H. Karpen. 2011. Assembly of
955 Drosophila centromeric chromatin proteins during mitosis. *PLoS Genet*. 7:e1002068.
956 Meraldi, P., V.M. Draviam, and P.K. Sorger. 2004. Timing and checkpoints in the regulation of mitotic
957 progression. *Dev Cell*. 7:45-60.
958 Moreno-Moreno, O., M. Torras-Llort, and F. Azorin. 2006. Proteolysis restricts localization of CID, the
959 centromere-specific histone H3 variant of Drosophila, to centromeres. *Nucleic Acids Res*. 34:6247-
960 6255.
961 Moyle, M.W., T. Kim, N. Hattersley, J. Espeut, D.K. Cheerambathur, K. Oegema, and A. Desai. 2014. A
962 Bub1-Mad1 interaction targets the Mad1-Mad2 complex to unattached kinetochores to initiate the
963 spindle checkpoint. *J Cell Biol*. 204:647-657.
964 Musacchio, A. 2015. The Molecular Biology of Spindle Assembly Checkpoint Signaling Dynamics. *Curr*
965 *Biol*. 25:R1002-1018.
966 Musacchio, A., and A. Desai. 2017. A Molecular View of Kinetochore Assembly and Function. *Biology*
967 *(Basel)*. 6.
968 Orr, B., H. Bousbaa, and C.E. Sunkel. 2007. Mad2-independent spindle assembly checkpoint
969 activation and controlled metaphase-anaphase transition in Drosophila S2 cells. *Mol Biol Cell*.
970 18:850-863.
971 Orr, B., and C.E. Sunkel. 2010. Drosophila CENP-C is essential for centromere identity. *Chromosoma*.
972 120:83-96.
973 Petsalaki, E., M. Dandoulaki, and G. Zachos. 2018. The ESCRT protein Chmp4c regulates mitotic
974 spindle checkpoint signaling. *J Cell Biol*. 217:861-876.
975 Przewloka, M.R., Z. Venkei, V.M. Bolanos-Garcia, J. Debski, M. Dadlez, and D.M. Glover. 2011. CENP-
976 C Is a Structural Platform for Kinetochore Assembly. *Curr Biol*. 21:399-405.
977 Przewloka, M.R., W. Zhang, P. Costa, V. Archambault, P.P. D'Avino, K.S. Lilley, E.D. Laue, A.D.
978 McAinsh, and D.M. Glover. 2007. Molecular analysis of core kinetochore composition and assembly
979 in Drosophila melanogaster. *PLoS One*. 2:e478.
980 Rahmani, Z., M.E. Gagou, C. Lefebvre, D. Emre, and R.E. Karess. 2009. Separating the spindle,
981 checkpoint, and timer functions of BubR1. *J Cell Biol*. 187:597-605.
982 Rothbauer, U., K. Zolghadr, S. Muyldermans, A. Schepers, M.C. Cardoso, and H. Leonhardt. 2008. A
983 versatile nanotrap for biochemical and functional studies with fluorescent fusion proteins. *Mol Cell*
984 *Proteomics*. 7:282-289.
985 Sacristan, C., M.U.D. Ahmad, J. Keller, J. Fermie, V. Groenewold, E. Tromer, A. Fish, R. Melero, J.M.
986 Carazo, J. Klumperman, A. Musacchio, A. Perrakis, and G.J. Kops. 2018. Dynamic kinetochore size
987 regulation promotes microtubule capture and chromosome biorientation in mitosis. *Nat Cell Biol*.
988 20:800-810.

989 Scaerou, F., I. Aguilera, R. Saunders, N. Kane, L. Blottiere, and R. Karess. 1999. The rough deal protein
990 is a new kinetochore component required for accurate chromosome segregation in Drosophila. *J Cell*
991 *Sci*. 112 (Pt 21):3757-3768.
992 Scaerou, F., D.A. Starr, F. Piano, O. Papoulas, R.E. Karess, and M.L. Goldberg. 2001. The ZW10 and
993 Rough Deal checkpoint proteins function together in a large, evolutionarily conserved complex
994 targeted to the kinetochore. *J Cell Sci*. 114:3103-3114.
995 Schittenhelm, R.B., F. Althoff, S. Heidmann, and C.F. Lehner. 2010. Detrimental incorporation of
996 excess Cenp-A/Cid and Cenp-C into Drosophila centromeres is prevented by limiting amounts of the
997 bridging factor Cal1. *J Cell Sci*. 123:3768-3779.
998 Schittenhelm, R.B., R. Chaleckis, and C.F. Lehner. 2009. Intrakinetochore localization and essential
999 functional domains of Drosophila Spc105. *EMBO J*. 28:2374-2386.
1000 Schittenhelm, R.B., S. Heeger, F. Althoff, A. Walter, S. Heidmann, K. Mechtler, and C.F. Lehner. 2007.
1001 Spatial organization of a ubiquitous eukaryotic kinetochore protein network in Drosophila
1002 chromosomes. *Chromosoma*. 116:385-402.
1003 Schmitt, H.D. 2010. Dsl1p/Zw10: common mechanisms behind tethering vesicles and microtubules.
1004 *Trends Cell Biol*. 20:257-268.
1005 Schramm, C., S. Elliott, A. Shevchenko, and E. Schiebel. 2000. The Bbp1p-Mps2p complex connects
1006 the SPB to the nuclear envelope and is essential for SPB duplication. *EMBO J*. 19:421-433.
1007 Silio, V., A.D. McAinsh, and J.B. Millar. 2015. KNL1-Bubs and RZZ Provide Two Separable Pathways for
1008 Checkpoint Activation at Human Kinetochores. *Dev Cell*. 35:600-613.
1009 Starr, D.A., R. Saffery, Z. Li, A.E. Simpson, K.H. Choo, T.J. Yen, and M.L. Goldberg. 2000. HZwint-1, a
1010 novel human kinetochore component that interacts with HZW10. *J Cell Sci*. 113 (Pt 11):1939-1950.
1011 Starr, D.A., B.C. Williams, T.S. Hays, and M.L. Goldberg. 1998. ZW10 helps recruit dynactin and
1012 dynein to the kinetochore. *J Cell Biol*. 142:763-774.
1013 Varma, D., X. Wan, D. Cheerambathur, R. Gassmann, A. Suzuki, J. Lawrimore, A. Desai, and E.D.
1014 Salmon. 2013. Spindle assembly checkpoint proteins are positioned close to core microtubule
1015 attachment sites at kinetochores. *J Cell Biol*. 202:735-746.
1016 Vleugel, M., E. Hoogendoorn, B. Snel, and G.J. Kops. 2012. Evolution and function of the mitotic
1017 checkpoint. *Dev Cell*. 23:239-250.
1018 Wainman, A., M.G. Giansanti, M.L. Goldberg, and M. Gatti. 2012. The Drosophila RZZ complex - roles
1019 in membrane trafficking and cytokinesis. *J Cell Sci*. 125:4014-4025.
1020 Westermann, S., and A. Schleiffer. 2013. Family matters: structural and functional conservation of
1021 centromere-associated proteins from yeast to humans. *Trends Cell Biol*. 23:260-269.
1022 Williams, B.C., and M.L. Goldberg. 1994. Determinants of Drosophila zw10 protein localization and
1023 function. *J Cell Sci*. 107 (Pt 4):785-798.
1024 Williams, B.C., T.L. Karr, J.M. Montgomery, and M.L. Goldberg. 1992. The Drosophila l(1)zw10 gene
1025 product, required for accurate mitotic chromosome segregation, is redistributed at anaphase onset.
1026 *J Cell Biol*. 118:759-773.
1027 Williams, B.C., Z. Li, S. Liu, E.V. Williams, G. Leung, T.J. Yen, and M.L. Goldberg. 2003. Zwilch, a new
1028 component of the ZW10/ROD complex required for kinetochore functions. *Mol Biol Cell*. 14:1379-
1029 1391.
1030 Wojcik, E., R. Basto, M. Serr, F. Scaerou, R. Karess, and T. Hays. 2001. Kinetochore dynein: its
1031 dynamics and role in the transport of the Rough deal checkpoint protein. *Nat Cell Biol*. 3:1001-1007.
1032 Zhang, G., T. Lischetti, D.G. Hayward, and J. Nilsson. 2015. Distinct domains in Bub1 localize RZZ and
1033 BubR1 to kinetochores to regulate the checkpoint. *Nat Commun*. 6:7162.

1034

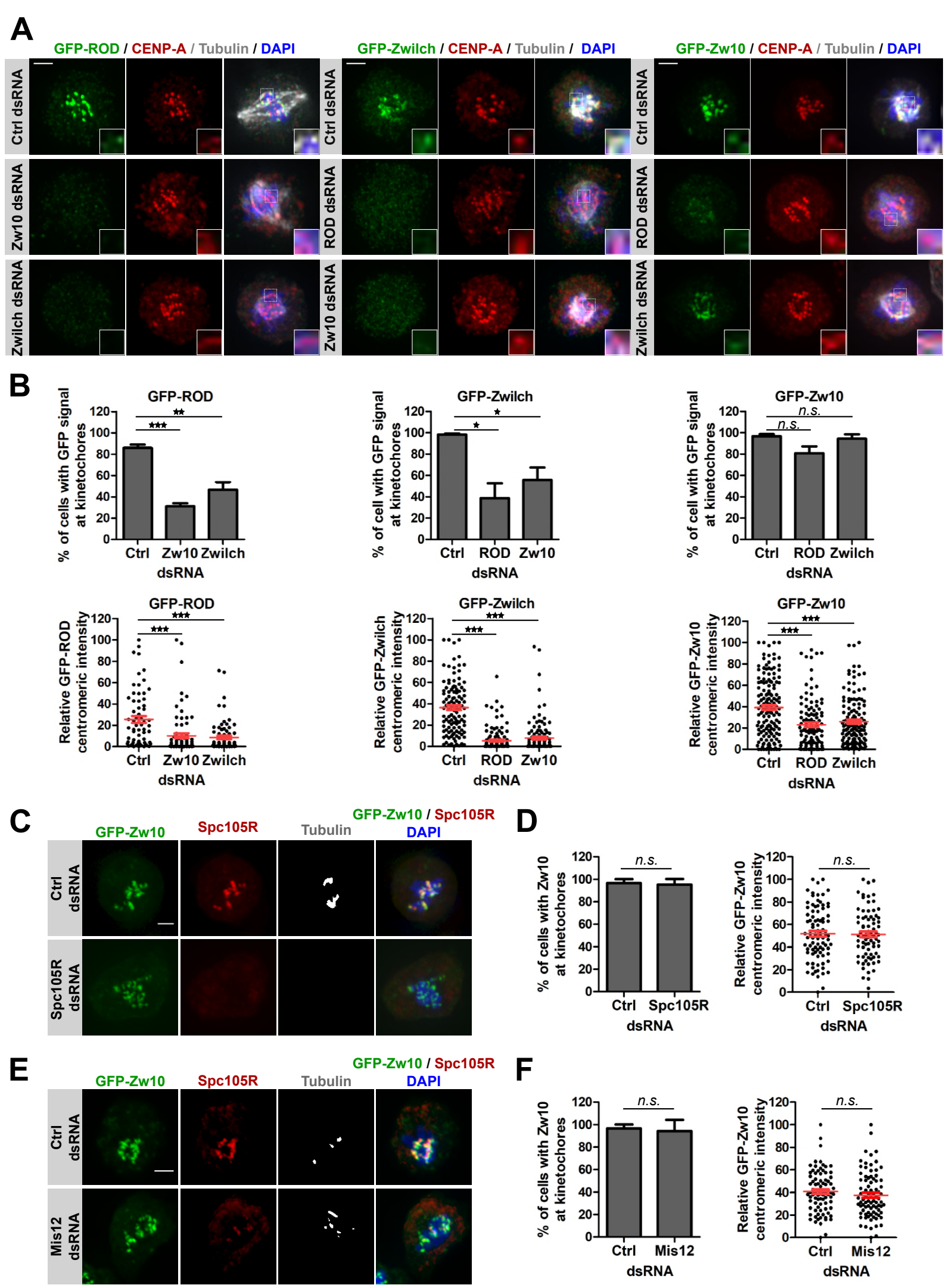
A
GFP-ROD / CENP-A / Tubulin / DAPI
GFP-Zwilch / CENP-A / Tubulin / DAPI
GFP-Zw10 / CENP-A / Tubulin / DAPI
Ctrl dsRNA
Zw10 dsRNA
Zwilch dsRNA
ROD dsRNA
B
GFP-ROD
GFP-Zwilch
GFP-Zw10
% of cells with GFP signal at kinetochores
% of cell with GFP signal at kinetochores
Relative GFP-ROD centromeric intensity
Relative GFP-Zwilch centromeric intensity
Relative GFP-Zw10 centromeric intensity
Ctrl
Zw10
Zwilch
ROD
dsRNA
n.s.
C
GFP-Zw10 / Spc105R
GFP-Zw10
Spc105R
Tubulin
DAPI
Ctrl dsRNA
Spc105R dsRNA
D
% of cells with Zw10 at kinetochores
Relative GFP-Zw10 centromeric intensity
Ctrl
Spc105R
dsRNA
n.s.
E
GFP-Zw10 / Spc105R
GFP-Zw10
Spc105R
Tubulin
DAPI
Ctrl dsRNA
Mis12 dsRNA
F
% of cells with Zw10 at kinetochores
Relative GFP-Zw10 centromeric intensity
Ctrl
Mis12
dsRNA
n.s.

Fig.1

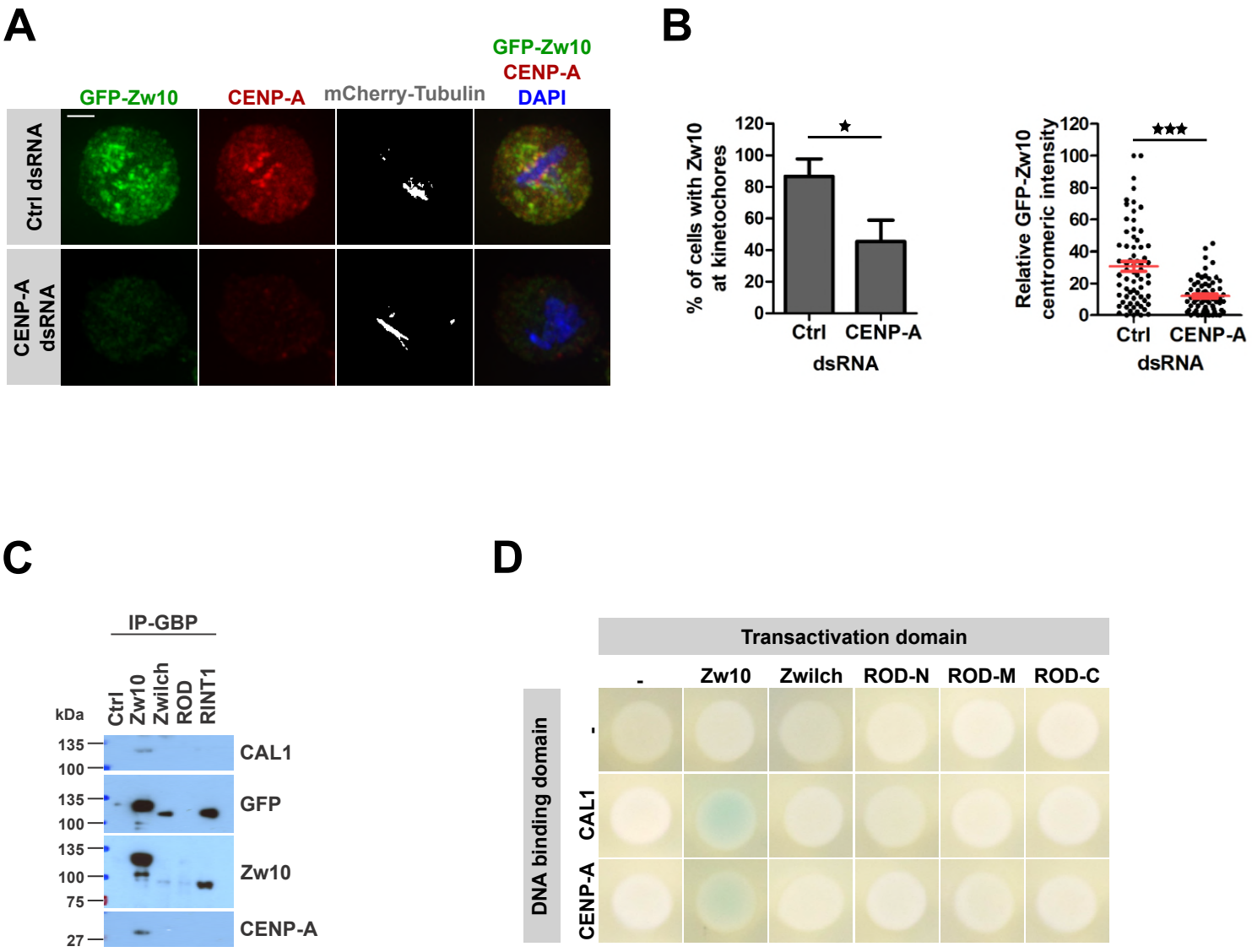
A
GFP-Zw10
CENP-A
mCherry-Tubulin
GFP-Zw10
CENP-A
DAPI
Ctrl dsRNA
CENP-A dsRNA
B
% of cells with Zw10 at kinetochores
120
100
80
60
40
20
0
*
Ctrl
CENP-A
dsRNA
Relative GFP-Zw10 centromeric intensity
120
100
80
60
40
20
0
***
Ctrl
CENP-A
dsRNA
C
IP-GBP
kDa
Ctrl
Zw10
Zwilch
ROD
RINT1
135
100
CAL1
135
100
GFP
135
100
75
Zw10
27
CENP-A
D
Transactivation domain
-
Zw10
Zwilch
ROD-N
ROD-M
ROD-C
DNA binding domain
-
CAL1
CENP-A

Fig.2

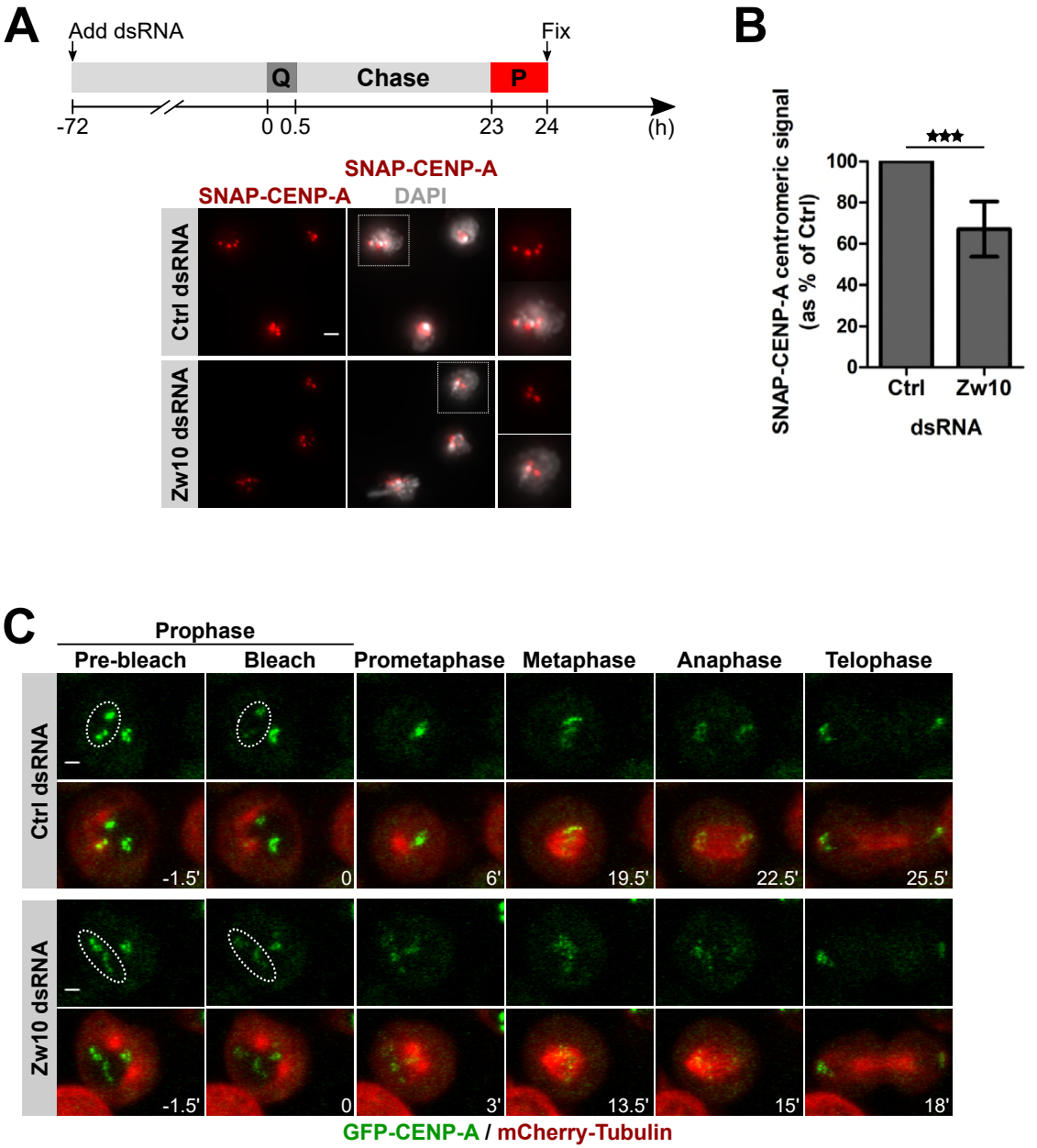
A
Add dsRNA
Fix
Q
Chase
P
-72
0 0.5
23
24
(h)
SNAP-CENP-A
SNAP-CENP-A
DAPI
Ctrl dsRNA
Zw10 dsRNA
B
SNAP-CENP-A centromeric signal (as % of Ctrl)
100
80
60
40
20
0
***
Ctrl
Zw10
dsRNA
C
Prophase
Pre-bleach
Bleach
Prometaphase
Metaphase
Anaphase
Telophase
Ctrl dsRNA
-1.5'
0
6'
19.5'
22.5'
25.5'
Zw10 dsRNA
-1.5'
0
3'
13.5'
15'
18'
GFP-CENP-A / mCherry-Tubulin
D
Ctrl dsRNA
Zw10 dsRNA
GFP-CENP-A centromeric signal
1.0
0.8
0.6
0.4
0.2
0.0
-1.5
0.0
1.5
3.0
4.5
6.0
7.5
9.0
10.5
12.0
13.5
15.0
16.5
18.0
19.5
21.0
22.5
24.0
25.5
27.0
28.5
30.0
Time (Min)
E
Recovery rate of GFP-CENP-A (a.u.)
0.010
0.008
0.006
0.004
0.002
0.000
n.s.
n=10
n=8
Ctrl
Zw10
dsRNA

Fig.3

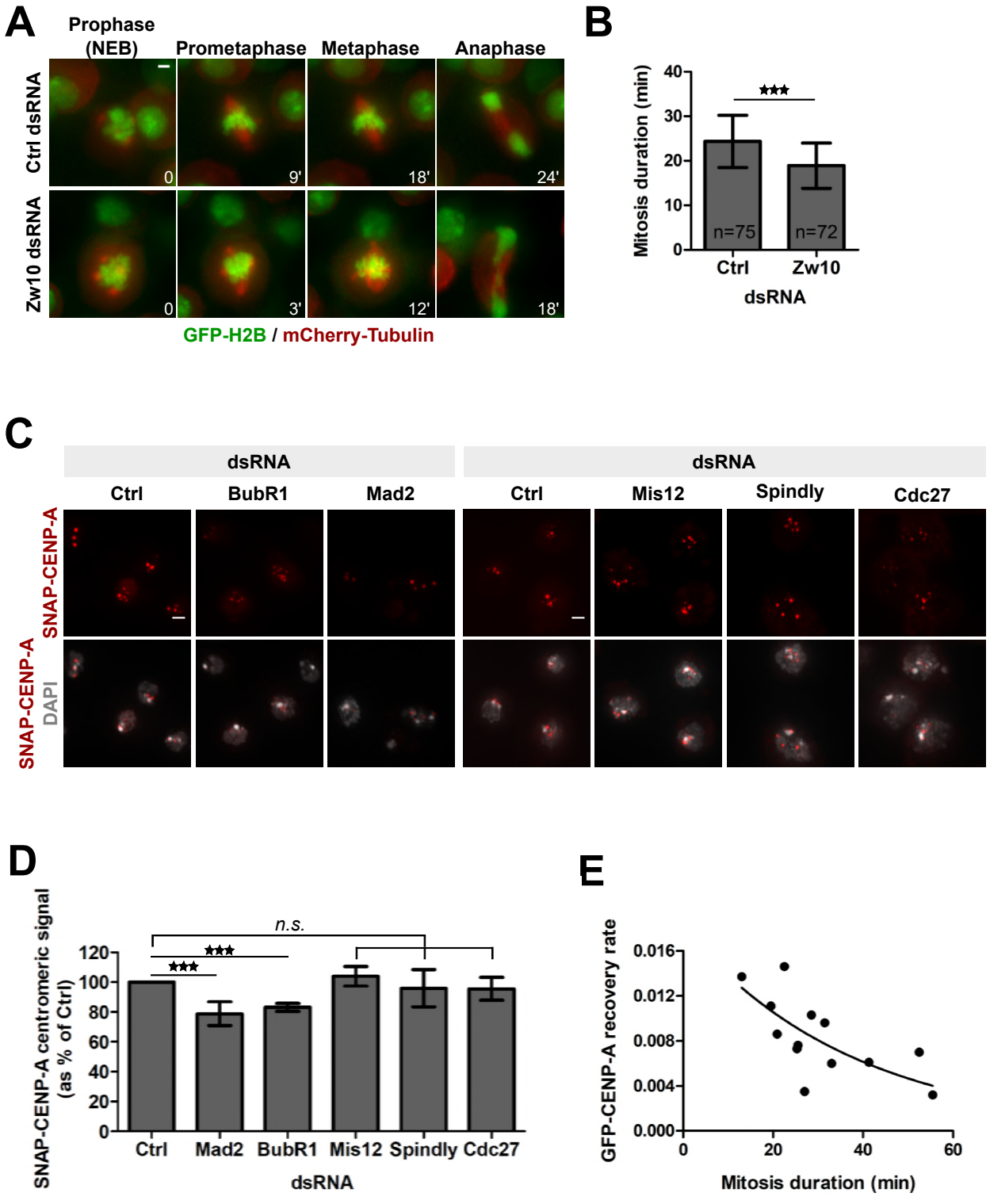
A
Prophase (NEB)
Prometaphase
Metaphase
Anaphase
Ctrl dsRNA
Zw10 dsRNA
0
9'
18'
24'
0
3'
12'
18'
GFP-H2B / mCherry-Tubulin
B
Mitosis duration (min)
40
30
20
10
0
***
n=75
n=72
Ctrl
Zw10
dsRNA
C
dsRNA
dsRNA
Ctrl
BubR1
Mad2
Ctrl
Mis12
Spindly
Cdc27
SNAP-CENP-A
SNAP-CENP-A
DAPI
D
SNAP-CENP-A centromeric signal (as % of Ctrl)
120
100
80
60
40
20
0
n.s.
***
***
Ctrl
Mad2
BubR1
Mis12
Spindly
Cdc27
dsRNA
E
GFP-CENP-A recovery rate
0.016
0.012
0.008
0.004
0.000
0
20
40
60
Mitosis duration (min)

Fig.4

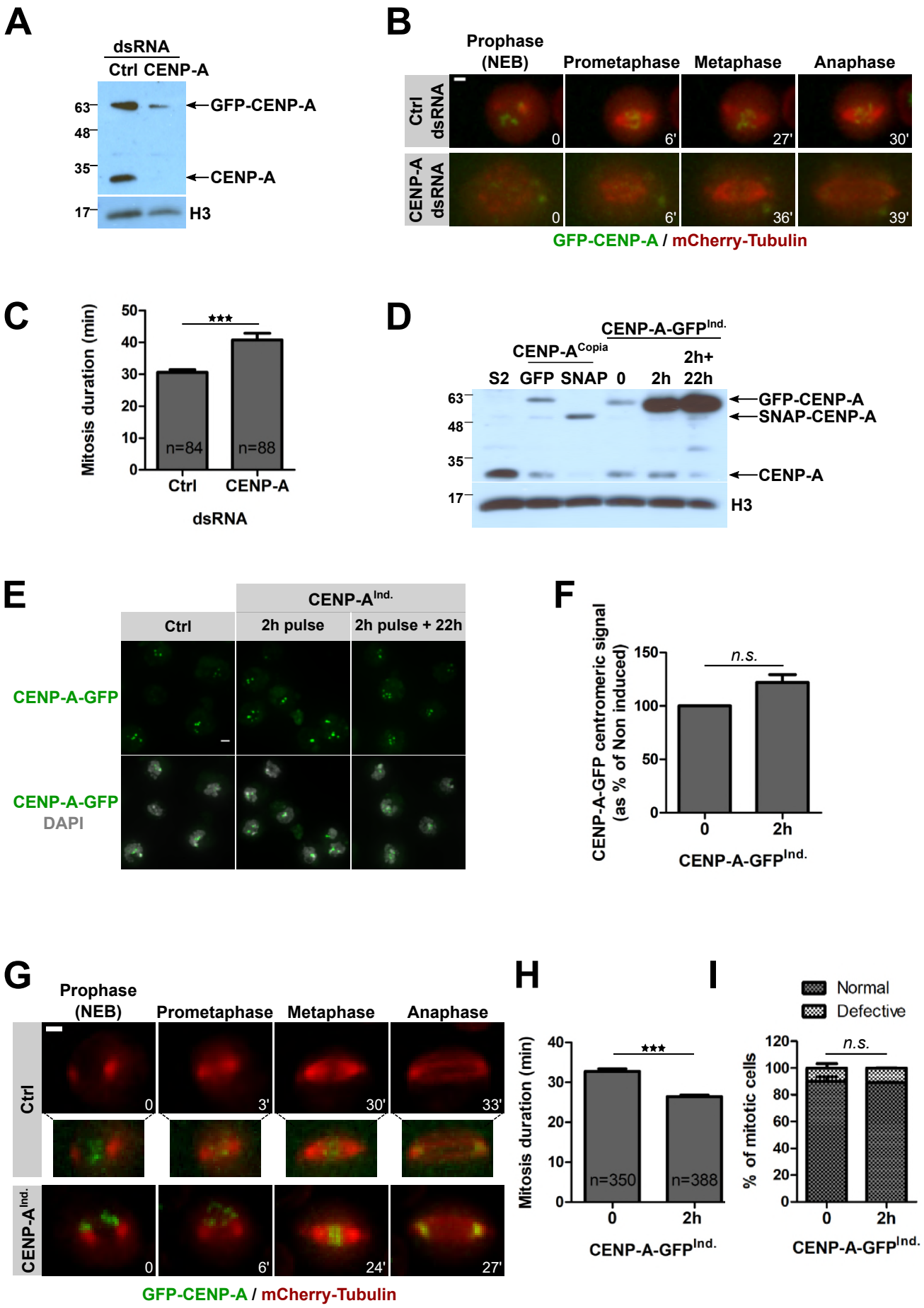
A
dsRNA
Ctrl CENP-A
63
48
35
17
GFP-CENP-A
CENP-A
H3
B
Prophase (NEB)
Prometaphase
Metaphase
Anaphase
Ctrl dsRNA
CENP-A dsRNA
0
6'
27'
30'
0
6'
36'
39'
GFP-CENP-A / mCherry-Tubulin
C
Mitosis duration (min)
50
40
30
20
10
0
***
n=84
n=88
Ctrl
CENP-A
dsRNA
D
CENP-A-GFP^Ind.
CENP-A^Copia
2h+
S2 GFP SNAP 0 2h 22h
63
48
35
17
GFP-CENP-A
SNAP-CENP-A
CENP-A
H3
E
CENP-A^Ind.
Ctrl
2h pulse
2h pulse + 22h
CENP-A-GFP
CENP-A-GFP
DAPI
F
CENP-A-GFP centromeric signal (as % of Non induced)
150
100
50
0
n.s.
0
2h
CENP-A-GFP^Ind.
G
Prophase (NEB)
Prometaphase
Metaphase
Anaphase
Ctrl
CENP-A^Ind.
0
3'
30'
33'
0
6'
24'
27'
GFP-CENP-A / mCherry-Tubulin
H
Mitosis duration (min)
40
30
20
10
0
***
n=350
n=388
0
2h
CENP-A-GFP^Ind.
I
Normal
Defective
% of mitotic cells
120
100
80
60
40
20
0
n.s.
0
2h
CENP-A-GFP^Ind.

Fig.5

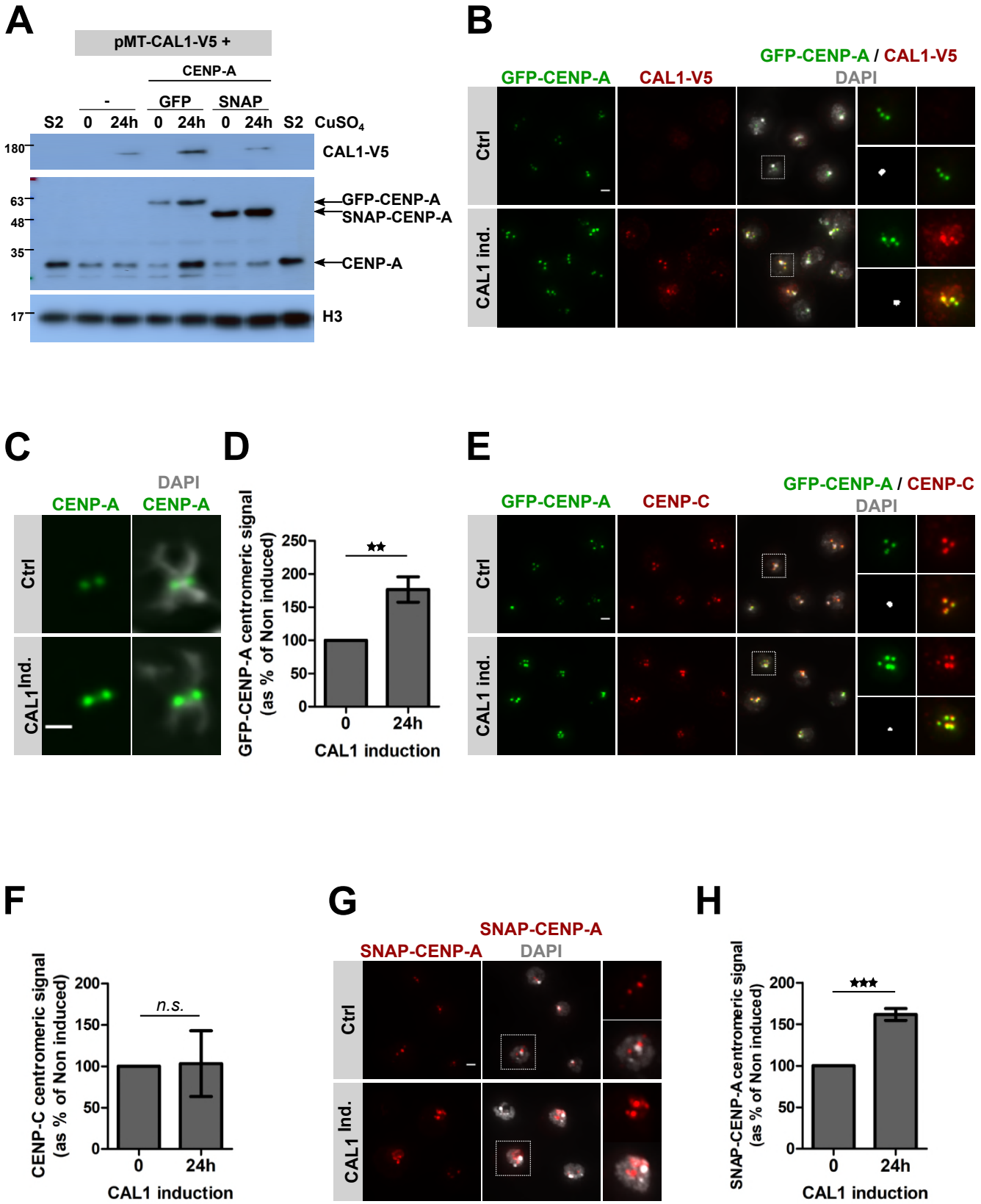
A
pMT-CAL1-V5 +
CENP-A
-
GFP
SNAP
S2 0 24h 0 24h 0 24h S2 CuSO4
180
CAL1-V5
63
48
35
GFP-CENP-A
SNAP-CENP-A
CENP-A
17
H3
B
GFP-CENP-A
CAL1-V5
GFP-CENP-A / CAL1-V5
DAPI
Ctrl
CAL1 ind.
C
CENP-A
DAPI
CENP-A
Ctrl
CAL1 Ind.
D
GFP-CENP-A centromeric signal (as % of Non induced)
250
200
150
100
50
0
**
0
24h
CAL1 induction
E
GFP-CENP-A
CENP-C
GFP-CENP-A / CENP-C
DAPI
Ctrl
CAL1 ind.
F
CENP-C centromeric signal (as % of Non induced)
200
150
100
50
0
n.s.
0
24h
CAL1 induction
G
SNAP-CENP-A
SNAP-CENP-A
DAPI
Ctrl
CAL1 Ind.
H
SNAP-CENP-A centromeric signal (as % of Non induced)
200
150
100
50
0
***
0
24h
CAL1 induction

Fig.6

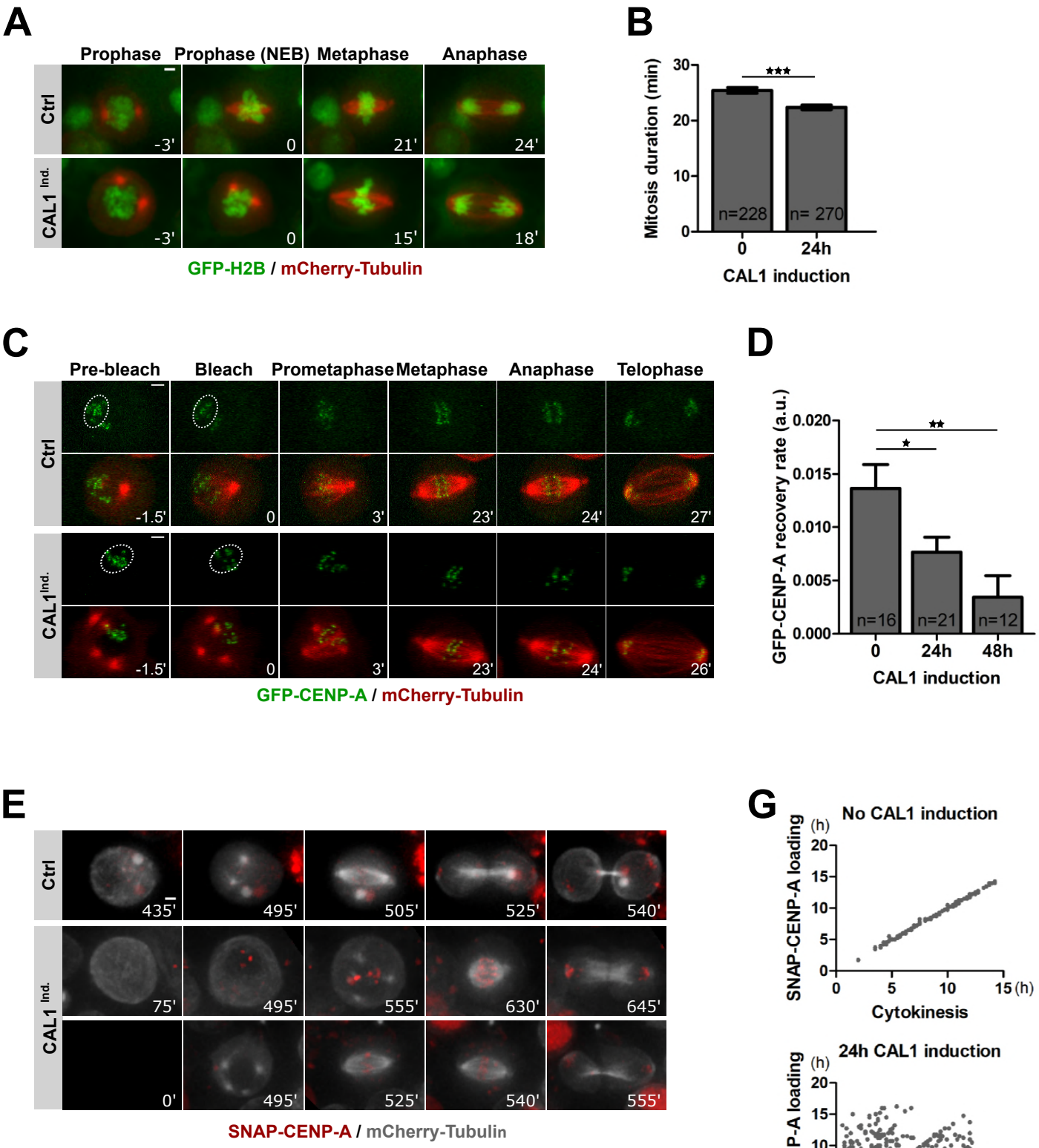

F

	Ctrl		CAL1 induction	
SNAP-CENP-A + cells	38 %	(167/452)	91 %	(371/458)
SNAP-CENP-A signal:				
Before Mitosis	0		31 %	(114/371)
During mitosis	91 %	(152/167)	18 %	(67/371)
After cytokinesis	9 %	(15/167)	51 %	(191/371)

Fig.7

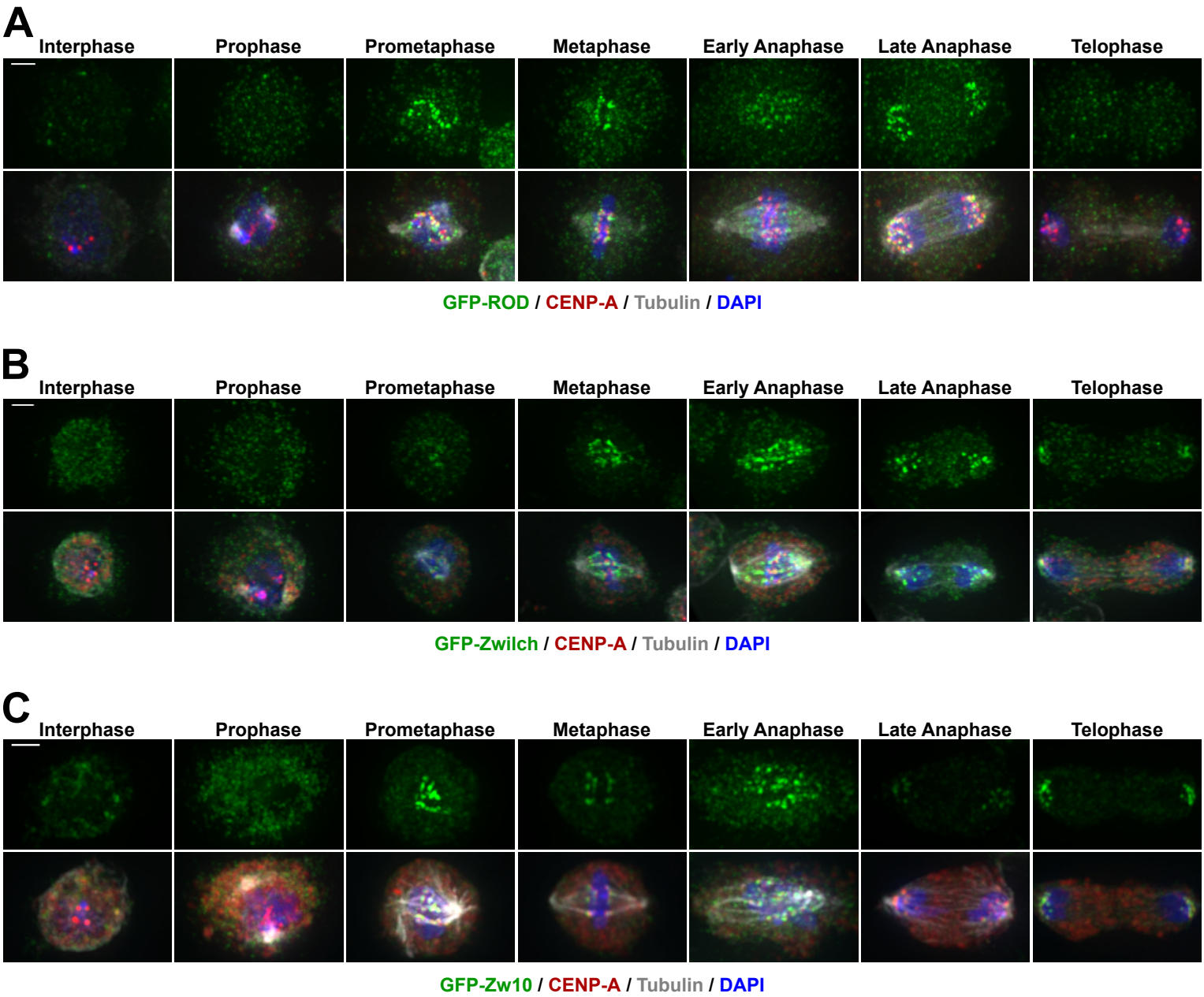
A
Interphase
Prophase
Prometaphase
Metaphase
Early Anaphase
Late Anaphase
Telophase
GFP-ROD / CENP-A / Tubulin / DAPI
B
Interphase
Prophase
Prometaphase
Metaphase
Early Anaphase
Late Anaphase
Telophase
GFP-Zwilch / CENP-A / Tubulin / DAPI
C
Interphase
Prophase
Prometaphase
Metaphase
Early Anaphase
Late Anaphase
Telophase
GFP-Zw10 / CENP-A / Tubulin / DAPI

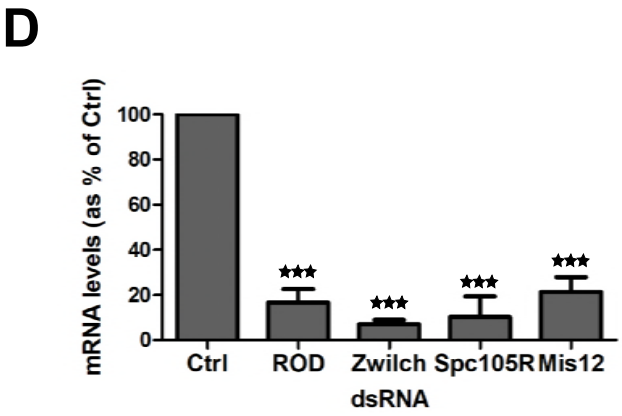
D
mRNA levels (as % of Ctrl)
100
80
60
40
20
0
***
***
***
***
Ctrl
ROD
Zwilch
Spc105R
Mis12
dsRNA

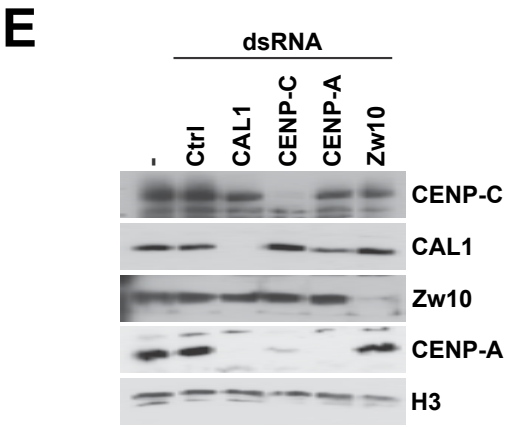
E
dsRNA
-
Ctrl
CAL1
CENP-C
CENP-A
Zw10
CENP-C
CAL1
Zw10
CENP-A
H3

Fig.S1

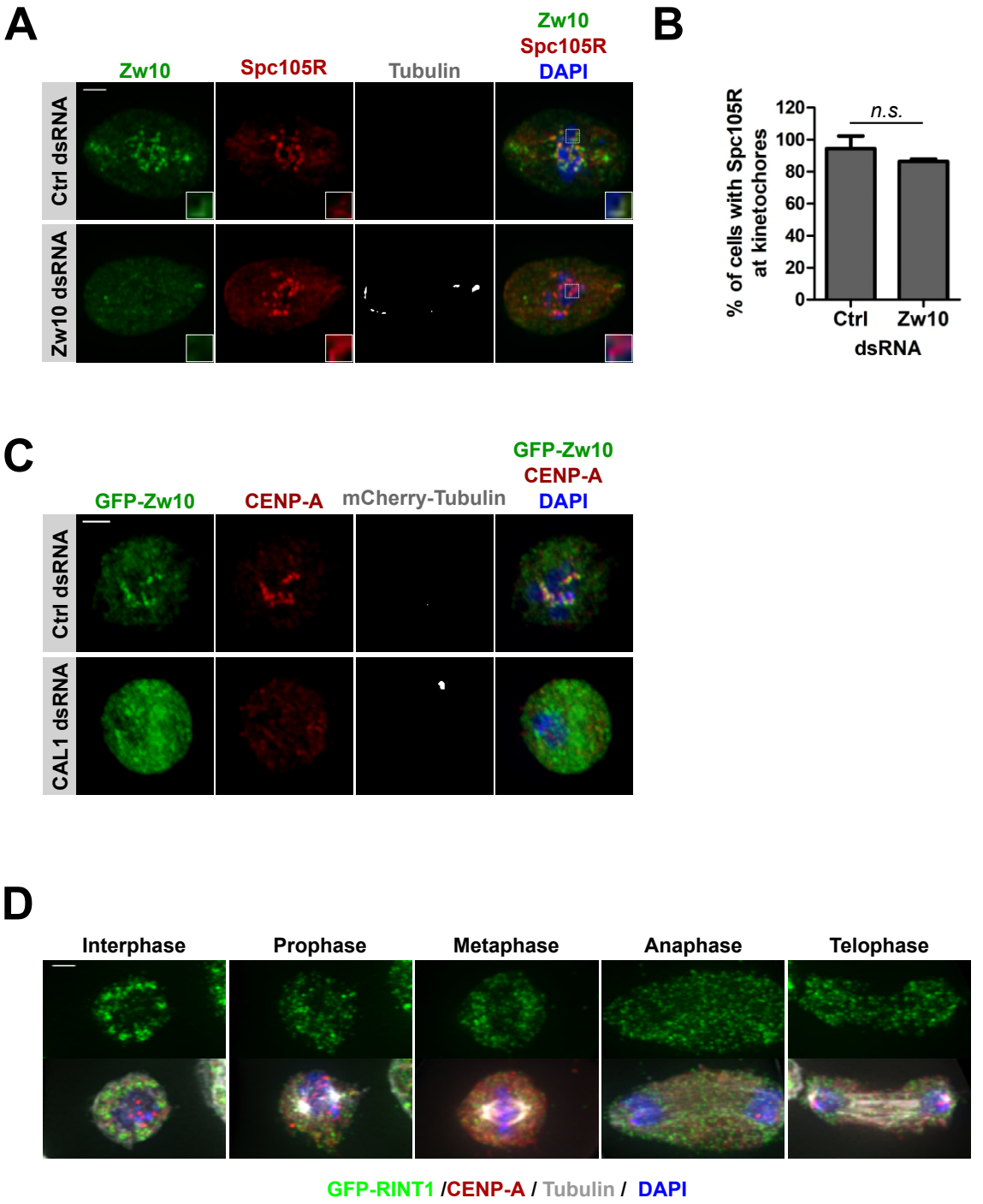
A
Zw10
Spc105R
Tubulin
Zw10
Spc105R
DAPI
Ctrl dsRNA
Zw10 dsRNA
B
% of cells with Spc105R at kinetochores
120
100
80
60
40
20
0
n.s.
Ctrl
Zw10
dsRNA
C
GFP-Zw10
CENP-A
mCherry-Tubulin
GFP-Zw10
CENP-A
DAPI
Ctrl dsRNA
CAL1 dsRNA
D
Interphase
Prophase
Metaphase
Anaphase
Telophase
GFP-RINT1 /CENP-A / Tubulin / DAPI
E
Transactivation domain
-
Zw10
Zw10482-721
Zw10241-481
Zw101-240
DNA binding domain
-
CAL1
CAL1680-979
CAL11-679
F
Zw10 BD
1
407
699
979
CAL1
CENP-A BD
CENP-C BD
RBS1
RBS2
RDX BD

Fig.S2

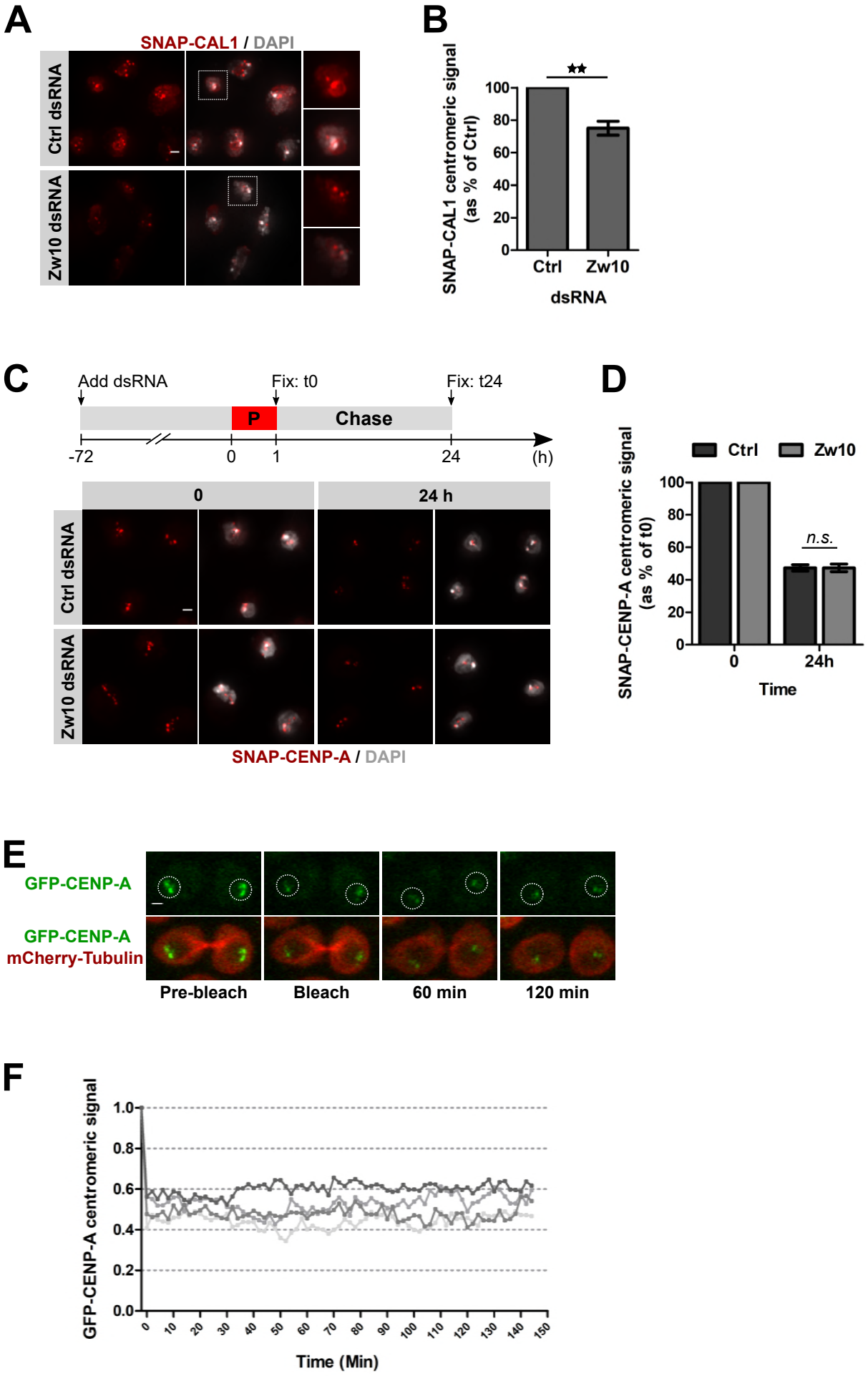
A
SNAP-CAL1 / DAPI
Ctrl dsRNA
Zw10 dsRNA
B
SNAP-CAL1 centromeric signal (as % of Ctrl)
100
80
60
40
20
0
Ctrl
Zw10
dsRNA
C
Add dsRNA
Fix: t0
Fix: t24
P
Chase
-72
0
1
24
(h)
0
24 h
Ctrl dsRNA
Zw10 dsRNA
SNAP-CENP-A / DAPI
D
Ctrl
Zw10
SNAP-CENP-A centromeric signal (as % of t0)
n.s.
0
24h
Time
E
GFP-CENP-A
GFP-CENP-A
mCherry-Tubulin
Pre-bleach
Bleach
60 min
120 min
F
GFP-CENP-A centromeric signal
1.0
0.8
0.6
0.4
0.2
0.0
0
10
20
30
40
50
60
70
80
90
100
110
120
130
140
150
Time (Min)

Fig.S3

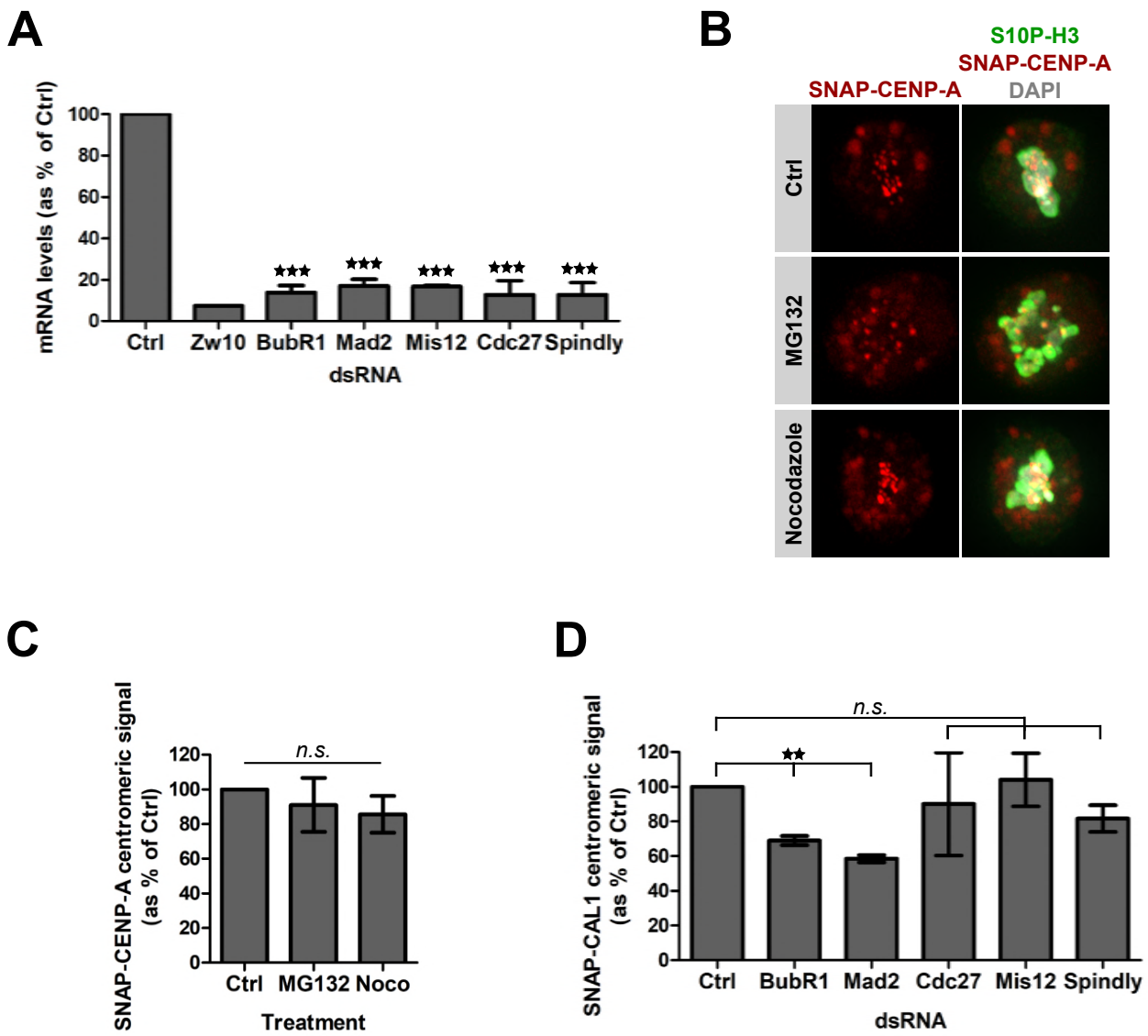
A
mRNA levels (as % of Ctrl)
100
80
60
40
20
0
***
Ctrl
Zw10
BubR1
Mad2
Mis12
Cdc27
Spindly
dsRNA
B
S10P-H3
SNAP-CENP-A
SNAP-CENP-A
DAPI
Ctrl
MG132
Nocodazole
C
SNAP-CENP-A centromeric signal (as % of Ctrl)
120
100
80
60
40
20
0
n.s.
Ctrl
MG132
Noco
Treatment
D
SNAP-CAL1 centromeric signal (as % of Ctrl)
n.s.
**
Ctrl
BubR1
Mad2
Cdc27
Mis12
Spindly
dsRNA

Fig.S4

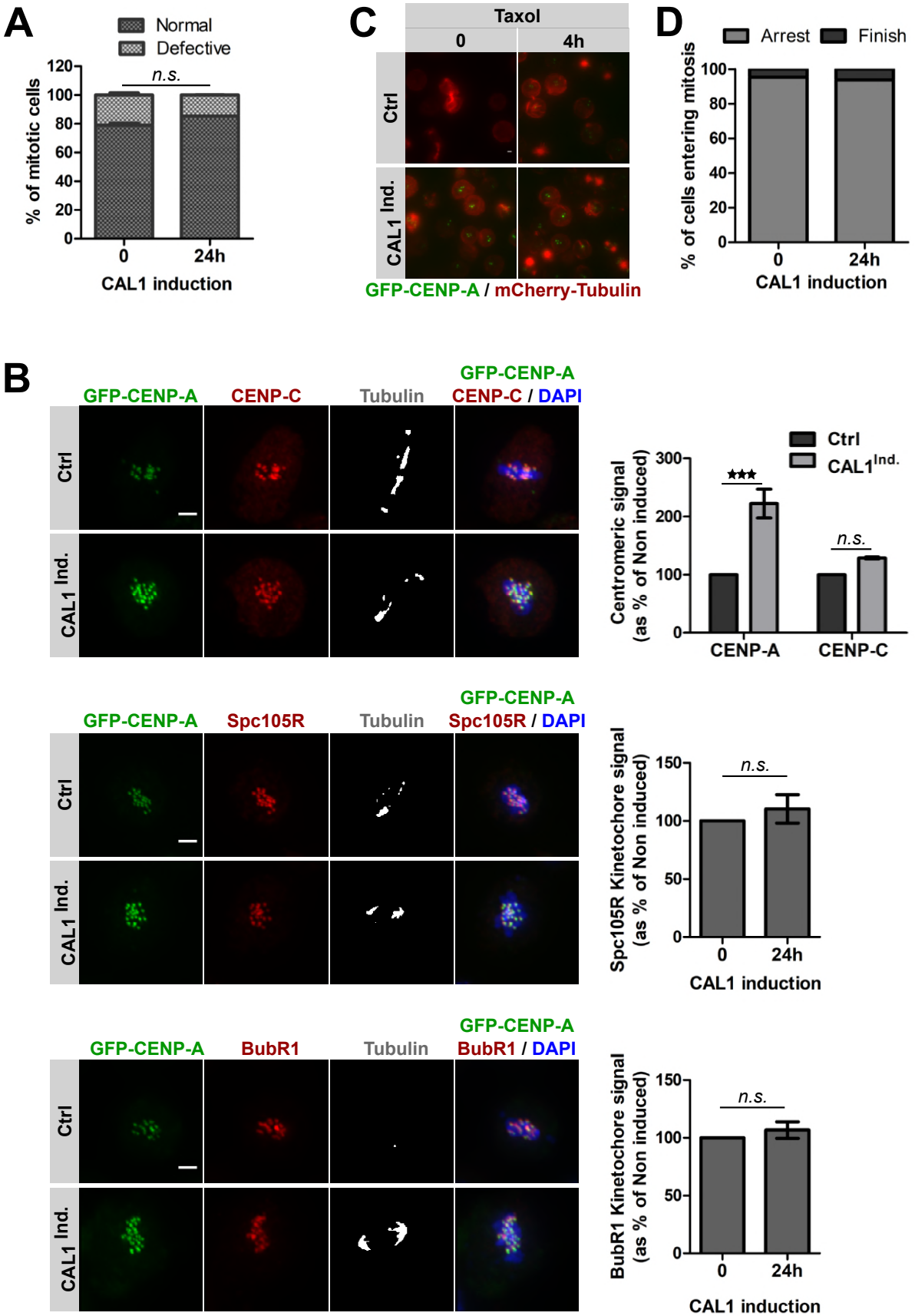
A
Normal
Defective
% of mitotic cells
120
100
80
60
40
20
0
n.s.
0
24h
CAL1 induction
C
Taxol
0
4h
Ctrl
CAL1 Ind.
GFP-CENP-A / mCherry-Tubulin
D
Arrest
Finish
% of cells entering mitosis
100
80
60
40
20
0
0
24h
CAL1 induction
B
GFP-CENP-A
CENP-C
Tubulin
GFP-CENP-A
CENP-C / DAPI
Ctrl
CAL1 Ind.
Centromeric signal
(as % of Non induced)
300
200
100
0
Ctrl
CAL1Ind.
***
n.s.
CENP-A
CENP-C
GFP-CENP-A
Spc105R
Tubulin
GFP-CENP-A
Spc105R / DAPI
Ctrl
CAL1 Ind.
Spc105R Kinetochore signal
(as % of Non induced)
150
100
50
0
n.s.
0
24h
CAL1 induction
GFP-CENP-A
BubR1
Tubulin
GFP-CENP-A
BubR1 / DAPI
Ctrl
CAL1 Ind.
BubR1 Kinetochore signal
(as % of Non induced)
150
100
50
0
n.s.
0
24h
CAL1 induction

Fig.S5

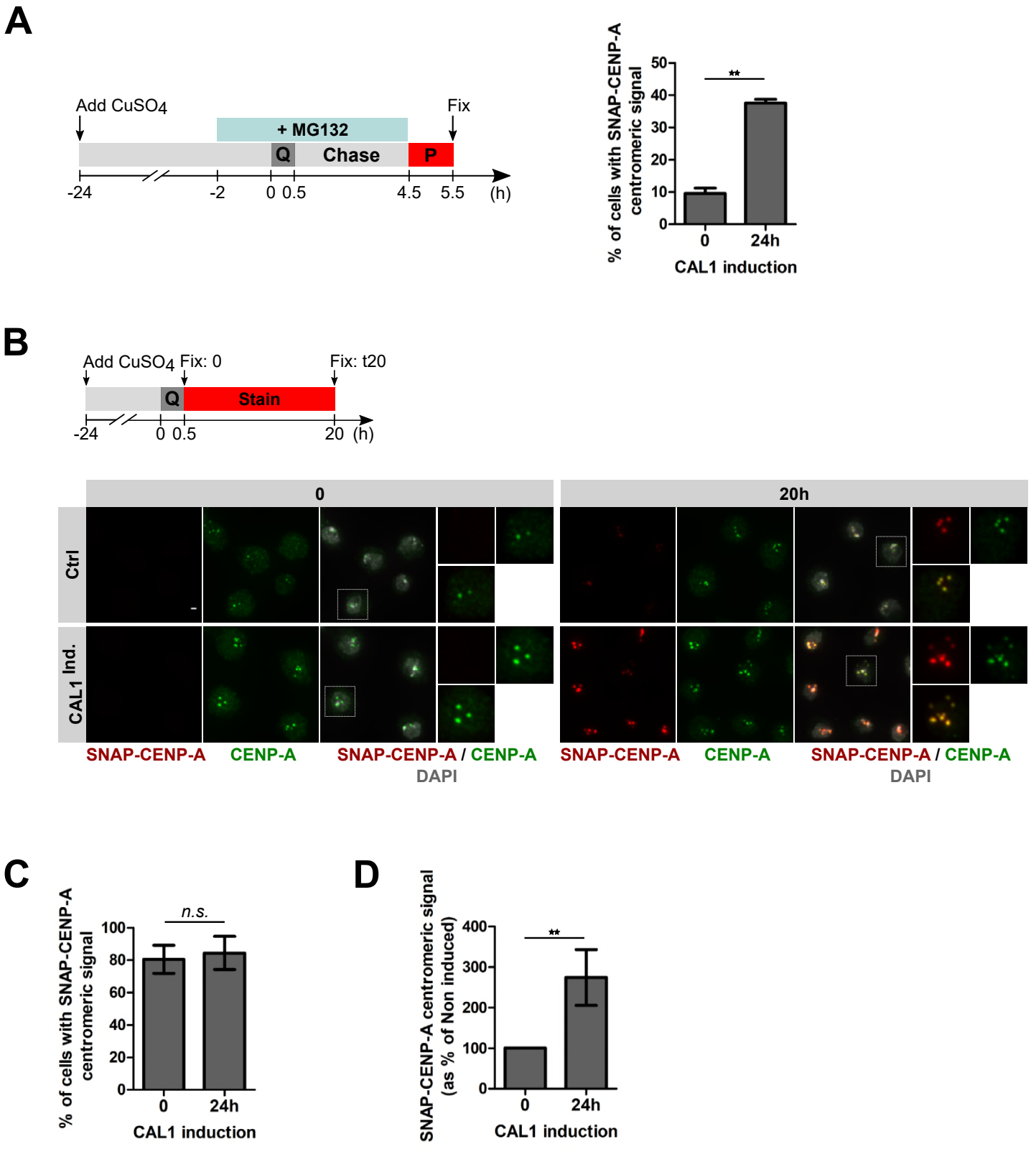
A
Add CuSO4
Fix
+ MG132
Q
Chase
P
-24
-2
0 0.5
4.5
5.5
(h)
% of cells with SNAP-CENP-A centromeric signal
50
40
30
20
10
0
**
0
24h
CAL1 induction
B
Add CuSO4
Fix: 0
Fix: t20
Q
Stain
-24
0 0.5
20
(h)
0
20h
Ctrl
CAL1 Ind.
SNAP-CENP-A
CENP-A
SNAP-CENP-A / CENP-A
DAPI
SNAP-CENP-A
CENP-A
SNAP-CENP-A / CENP-A
DAPI
C
% of cells with SNAP-CENP-A centromeric signal
100
80
60
40
20
0
n.s.
0
24h
CAL1 induction
D
SNAP-CENP-A centromeric signal (as % of Non induced)
400
300
200
100
0
**
0
24h
CAL1 induction

Fig.S6